Theory of Input Spike Auto- and Cross-Correlations and Their Effect on the Response of Spiking Neurons

Rubén Moreno-Bote*
rmoreno@cns.nyu.edu
Alfonso Renart[†]
arenart@andromeda.rutgers.edu
Néstor Parga
nestor.parga@uam.es
Departamento de Física Teórica. Universidad Autónoma de Madrid, Cantoblanco 28049, Madrid, Spain

Spike correlations between neurons are ubiquitous in the cortex, but their role is not understood. Here we describe the firing response of a leaky integrate-and-fire neuron (LIF) when it receives a temporally correlated input generated by presynaptic correlated neuronal populations. Input correlations are characterized in terms of the firing rates, Fano factors, correlation coefficients, and correlation timescale of the neurons driving the target neuron. We show that the sum of the presynaptic spike trains cannot be well described by a Poisson process. In fact, the total input current has a nontrivial two-point correlation function described by two main parameters: the correlation timescale (how precise the input correlations are in time) and the correlation magnitude (how strong they are). Therefore, the total current generated by the input spike trains is not well described by a white noise gaussian process. Instead, we model the total current as a colored gaussian process with the same mean and two-point correlation function, leading to the formulation of the problem in terms of a Fokker-Planck equation. Solutions of the output firing rate are found in the limit of short and long correlation timescales. The solutions described here expand and improve on our previous results (Moreno, de la Rocha, Renart, & Parga, 2002) by presenting new analytical expressions for the output firing rate for general IF neurons, extending the validity of the results for arbitrarily large correlation magnitude, and by describing the differential effect of correlations on the mean-driven or noise-dominated firing regimes. Also the details of this novel formalism are given here for the first time. We employ numerical simulations to

---

*Rubén Moreno-Bote is currently at the Center for Neural Science, New York University, New York, NY 10003, U.S.A.

[†]Alfonso Renart is currently at the Center for Molecular and Behavioral Neuroscience, Rutgers, State University of New Jersey, Newark, NJ 07102, U.S.A.

confirm the analytical solutions and study the firing response to sudden changes in the input correlations. We expect this formalism to be useful for the study of correlations in neuronal networks and their role in neural processing and information transmission.

1 Introduction

A major problem in neuroscience is understanding the way neurons communicate with each other. Because neurons in the cortex are densely connected and share common inputs (White, 1989; Braitenberg & Schüz, 1991), some degree of correlation between their discharges is unavoidable. Indeed, correlations in the spiking activity of neurons are routinely observed throughout the cortex (Zohary, Shadlen, & Newsome, 1994; deCharms & Merzenich, 1996; Lee, Port, Kruse1, & Georgopoulos, 1998; Usrey & Reid, 1999; Bair, Zohary, & Newsome, 2001; for a review see Salinas & Sejnowski, 2001 and Averbeck & Lee, 2004). Correlations could have an important functional role, as the temporal synchronization of neuronal activity has been shown to correlate with particular states of behaving animals (Vaadia et al., 1995; Riehle, Grun, Diesmann, & Aertsen, 1997; Fries, Roelfsema, Engel, König, & Singer, 1997; Steinmetz et al., 2000; Fries, Reynolds, Rorie, & Desimone, 2001). From a more traditional point of view, correlations have been considered as a coding dimension independent of the firing rate (deCharms & Merzenich, 1996; Wehr & Laurent, 1999; Laurent, 2001). However, it remains controversial whether correlated activity has a role in coding, or whether its main role is as a gating mechanism of the flow of information in cortical circuits (Salinas & Sejnowski, 2001; Averbeck & Lee, 2004).

Before the functional role of correlations can be addressed, a primary question to solve is how correlations affect the firing properties of neurons. Previous work in this direction has revealed that neurons can be very sensitive even to weak correlations in their inputs (Burkitt & Clark, 1999; Feng & Brown, 2000; Salinas & Sejnowski, 2000). However, in most of these studies, only zero time lag correlated inputs (perfect synchronization) has been used. This means that when one spike arrives at one presynaptic terminal, another spike is more likely to be found at the same time in another presynaptic terminal. This perfect synchrony is not expected to be exhibited by real neuronal systems, given their finite temporal precision. Instead, synchrony with a nonzero time precision τ_c seems to be the realistic case, with $\tau_c \sim 15$ ms in monkey primary auditory cortex (deCharms & Merzenich, 1996), $\tau_c \sim 5$ ms in primary visual cortex of strabismic cats (Fries et al., 1997) (in this case the cross-correlogram is accompanied by an oscillatory pattern), τ_c with very broad values ranging from less than 15 ms to more than 200 ms mediating interactions between areas V1 and V2 in monkeys (Nowak, Munk, James, Girard, & Bullier, 1999), or $\tau_c \sim 10$ ms in the monkey visual area MT (Bair et al., 2001). In this case, if a spike arrives at time $t = 0$

at a presynaptic terminal, another spike is more, or less, likely than the chance level determined by the firing rate to arrive within a time τ_c around $t = 0$ at another (or the same) terminal.

We have shown previously (Moreno, de la Rocha, Renart, & Parga, 2002) that the total current to a neuron generated by exponentially correlated afferent spike trains can be described (among other parameters) by the correlation time, τ_c, and the correlation magnitude, α (see definitions in section 3). Each parameter carries important information about the characteristics of the input correlations (either temporal or intensity information). Intuitively, a short correlation time τ_c means that afferent spikes synchronize within short time windows of size τ_c. Decreasing τ_c will enhance the temporal precision of correlations. The correlation magnitude, α, roughly represents how many spikes are expected above chance in a time window τ_c given that there was a spike centered in that time window. Therefore, it is a measure of the intensity of the correlations. For uncorrelated spike trains, $\alpha = 0$, while for positively correlated spike trains, $\alpha > 0$, and for negatively correlated, $\alpha < 0$. As we will show, the correlation time and magnitude can also be related to the autocorrelograms (ACGs) and cross-correlograms (CCGs) of recorded spike trains. The correlation time measures the typical width of the CCG, while the correlation magnitude is proportional to the area under the CCG curve.

Both τ_c and α can affect the neuron's firing response in complicated ways. Separating their effects was crucial in our previous work (Moreno et al., 2002), where the effects of changing the timescale and the magnitude of the input correlations could be studied independently. In particular, one of the main qualitative results was that if α is kept constant, neurons are sensitive to input correlations only when the correlation time is shorter than the membrane time constant.[1]

The main problem studied in this article is schematized in Figure 1 and can be summarized as follows. What is the effect of the magnitude and the timescale of the input spike correlations on the neuron firing response? We answer this question by addressing consecutively several subproblems. First, after presenting the model in section 2, we describe in section 3 the statistical properties of the afferent spike trains that drive a leaky integrate-and-fire (LIF) neuron. The spike trains are characterized in terms of their firing rates, Fano factors, correlation coefficients, and correlation timescale and are assumed to have exponential auto- and cross-correlations. Correlated and uncorrelated Poisson spike trains are just special cases of these. The total current generated by the sum of the spike trains is described up

---

[1]This mechanism is consistent with coincidence detection (Abeles, 1982; Bernander, Douglas, Martin, & Koch, 1991; Softky & Koch, 1993; Softky, 1994). Note, however, that these authors consider input spike coincidence detection in the submillisecond range, while our results more generally concern the effect of correlation timescale of any size on a neuron with any membrane time constant.
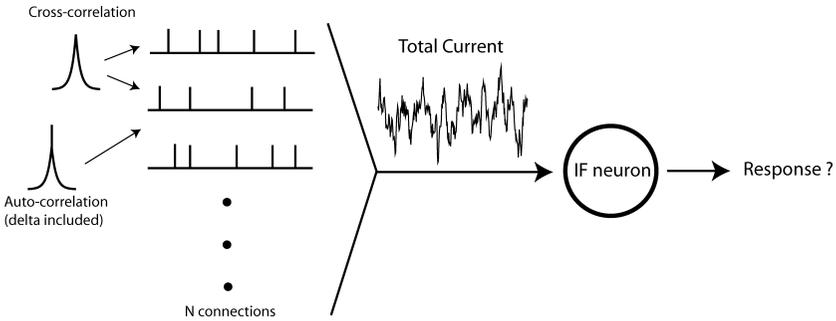
Figure 1: Illustration of the problem studied in this article (a fully detailed description is given in the text). A set of afferent presynaptic spike trains impinges on an integrate-and-fire neuron. Each individual spike train has exponentially shaped autocorrelations, describing the joint probability density of having two spikes separated by a particular time lag (a delta function should be included at zero time lag because the train is made of point events; see text). A fraction of the trains also have exponential cross-correlations, describing nonindependent firing of some of the presynaptic neurons. The total current generated by the presynaptic bombardment is replaced by a gaussian process with the same mean and two-point correlation function as those generated by the superposition of all presynaptic spike trains. The goal is to characterize the spiking response properties of the LIF neuron as a function of the global magnitude and timescale of the input correlations.

to second-order statistics (the two-point correlation function) and shows exponential correlations (see section 3.2). Second, to solve the difficulties presented by the non-Markovian character of the input statistics, we seek to transform this input into a colored gaussian input with the same mean and two-point correlation function as those generated by the original current. Two different Markovian stochastic processes that generate this colored gaussian input are found in section 4. Then we obtain the Fokker-Plank equations (FPEs) associated with each of these two processes and the voltage of the neuron (see sections 4.1 and 4.2). Third, the output firing rate is obtained by solving the FPEs in the limits of short and long values of the correlation timescale compared to the membrane time constant of the neuron (see section 5). At this point we give a brief summary of the analytical expressions and their ranges of validity in section 6 and Table 1. An interpolation is then employed to join the two limits, and the analytical results are compared with numerical simulations in section 7.1. Finally, in section 7.2, we also show that neurons can track fast changes in input correlations. In section 8, we summarize the main results and discuss possible applications. Several computational details are provided in the appendixes.

Some of these results have been previously published in a brief format (Moreno et al., 2002). In this article, we extend the analytical techniques, obtain new results, and present a more pedagogical version of our work to facilitate the use of the mathematical expressions as well as the understanding of their derivation. In particular, a more general expression for the output firing rate is found in the presence of exponentially correlated input spike trains that is valid for long τ_c and for all positive α (see section 5.2). If the limit of small α is taken, this new expression becomes that found in Moreno et al. (2002) in the case of long τ_c, and therefore generalizes and extends the latter for large correlation magnitudes. The effect of input correlations in the mean-driven and noise-dominated input regimes is found to be different, and those peculiarities are discussed in section 7.1.

2 Model

We consider an LIF neuron with membrane potential $V(t)$ and membrane time constant τ_m. In the absence of input, the voltage decays exponentially toward the resting potential (here $V = 0$). In the presence of the synaptic current, $I(t)$, the membrane potential evolves according to

$$\dot{V}(t) = -\frac{V(t)}{\tau_m} + I(t) . \tag{2.1}$$

In the model, a spike is generated whenever the membrane potential $V(t)$ reaches a threshold value Θ. Following the spike, the potential is reset to a value H, from where, after an absolute refractory period τ_{ref}, the neuron can start integrating the synaptic current again.

We work in the limit of infinitely fast synaptic time constants, in which individual synaptic currents are represented by delta functions. Thus, the afferent current $I(t)$ is

$$I(t) = J_E \sum_{i=1}^{N_E} \sum_k \delta\left(t - t_i^k\right) - J_I \sum_{j=1}^{N_I} \sum_l \delta\left(t - t_j^l\right), \tag{2.2}$$

where $t_{i(j)}^{k(l)}$ represents the arrival time of the kth (lth) spike from the ith excitatory (jth inhibitory) presynaptic neuron, and $N_{E(I)}$ and $J_{E(I)}$ represent, respectively, the number of inputs and the size of the postsynaptic potentials from the excitatory (inhibitory) afferent populations.

We are interested in the case of stationary input statistics, so that the input firing rates do not depend on time (but see our simulation results for the case on nonstationary statistics in section 7.2). Therefore, assuming that the excitatory and inhibitory presynaptic neurons fire at rates ν_E and ν_I,

respectively, the mean current $\langle I(t) \rangle$ is computed as

$$\mu = \langle I(t) \rangle = N_E \, J_E \, \nu_E - N_I \, J_I \, \nu_I. \tag{2.3}$$

This result is independent of the statistics of the afferent spike trains. For example, the mean current generated by correlated or independent Poisson spike trains is exactly the same, provided that the processes are stationary and described by the same firing rates. However, the second-order statistics of the current will be very sensitive to the second-order statistical properties of the individual spike trains (e.g., their pair-wise correlations). In the next section, we determine the two-point correlation function in terms of the statistical properties of the presynaptic spike trains.

3 Second-Order Statistical Properties of the Current

3.1 Autocorrelograms. This section is devoted to the description of the second-order statistical properties of each individual spike train impinging on the LIF neuron. In the next section, we consider the second-order statistical properties of pairs of those spike trains. Here, we first define the Fano factor of the spike count of each input train. Then we introduce the autocorrelation function in the case of an exponentially correlated spike train. Finally, we show that the parameters defining the exponential autocorrelation function can be expressed in terms of the firing rate, Fano factor, and correlation time of the spike train.

Most theoretical models have considered afferent spike trains (see equation 2.2) as stochastic Poisson processes (see, e.g., Ricciardi, 1977; Tuckwell, 1988; Brunel & Sergi, 1998; Feng & Brown, 2000; Nykamp & Tranchina, 2001; LaCamera, Rauch, Luscher, Senn, & Fusi, 2004; Richardson & Gerstner, 2005). In this work, we relax this assumption. The Fano factor is often used to quantify the reliability of neuronal discharge. The Fano factor of the spike count in a time window T is defined as the ratio between the variance of the spike count and the mean number of spikes in that time window, that is,

$$F_N(T) = \frac{\sigma_N^2(T)}{\langle N(T) \rangle} = \frac{\langle (N(T) - \langle N(T) \rangle)^2 \rangle}{\langle N(T) \rangle}, \tag{3.1}$$

where $N(T)$ is the number of spikes counted in the time window T in each trial and brackets denote an average over trials. Note that in practice, the mean and variance can also be computed using a single long spike train (with stationary firing rate) obtained in a single trial, where now the average is obtained using nonoverlapping consecutive time windows instead of several trials. In either case, typically the time window T is taken to be large, so that at least tens of spikes are observed on average. A

Poisson spike train has a Fano factor equal to one. However, Fano factors calculated from spike trains obtained from electrophysiological recordings in vivo usually exceed one, laying in the interval $F_N \sim 1 - 1.5$ throughout the cerebral cortex (Dean, 1981; Softky & Koch, 1993; Albright, 1993; Shadlen & Newsome, 1998; Compte et al., 2003), which is inconsistent with the Poisson hypothesis (see also Amarasingham, Chen, German, Harrison, & Sheinberg, 2006).

Another important second-order statistical property of individual spike trains is the joint probability density of having spikes belonging to that same spike train at two times, t and t', denoted $P(t, t')$. In fact, from it one can derive any other second-order statistical quantity, such as the Fano factor (see below). For a Poisson spike train with rate ν, $P(t, t')$ is a delta function at zero-time lag and flat otherwise, as

$$P_{Poisson}(t, t') = \nu \delta(t - t') + \nu^2 . \tag{3.2}$$

The delta function at $t = t'$ serves to define $P(t, t')$ at all times; trivially, the probability density of having a spike at time t and a spike at time $t' = t$ is just the delta multiplied by the spike rate in that train, $\nu \delta(t - t')$; in other words, the presence of one spike is informative of the presence of a spike at that time (the same spike). For nonzero time lags ($t \neq t'$), this probability is the product of the probability densities of having spikes at two different times, that is, ν^2. For a general spike train, we define the autocorrelation function as the quantity

$$C(t, t') = P(t, t') - \nu^2, \tag{3.3}$$

that is, the joint probability density of having spikes at times t and t', from which the probability of finding them by chance (i.e., the rate to the square) is subtracted.

While Poisson trains have an autocorrelation with a single delta function at time lag zero and zero otherwise (i.e., $C_{Poisson}(t, t') = \nu \delta(t - t')$), autocorrelograms obtained from electrophysiological recordings show a decaying peak at nonzero time lags (disregarding refractory effects), sometimes together with a damped oscillatory pattern. A centered decaying peak in an autocorrelogram means that spikes tend to occur close together in time, forming groups of several spikes. Experimental autocorrelograms with a single peak and without oscillations can be fitted to an exponential function (e.g., Bair et al., 2001). We therefore consider stochastic spike trains with exponential autocorrelations with timescale τ_c,

$$C_p(t, t') \equiv \left\langle \left(\sum_k \delta(t - t_i^k) - \nu_p \right) \left(\sum_{k'} \delta(t' - t_i^{k'}) - \nu_p \right) \right\rangle$$

$$= \left\langle \sum_{k,k'} \delta\left(t - t_i^k\right)\delta\left(t' - t_i^{k'}\right) \right\rangle - \nu_p^2$$

$$= \nu_p \delta(t - t') + \nu_p \left(\frac{F_p - 1}{2\tau_c} \right) e^{-\frac{|t-t'|}{\tau_c}}, \tag{3.4}$$

as illustrated in Figure 2B. Since we assume that the input statistics are stationary, the input firing rates are time independent and the autocorrelation function depends on only time through the quantity $|t - t'|$. Here $p = E, I$; ν_p and F_p are the firing rate and the Fano factor of the spike count (for infinitely long time windows) of the individual trains coming from population p.[2] The connected two-point correlation function defined above is the joint probability density of finding one spike at time t and another at t' within the same spike train, from where the probability of observing them by chance, ν_p^2, is subtracted. Note that this function has two contributions: a delta function at zero time lag, coming from the fact that spikes are point events, and an exponential dependence measuring the excess probability of finding a spike at t' when it is known that there is another spike at t. While normally spikes in the same train are positively correlated ($F_N > 1$), the autocorrelogram in equation 3.4 also describes uncorrelated ($F_N = 1$, Poisson) and negatively correlated spikes ($F_N < 1$). With the parameterization we have chosen, fixing the Fano factor and changing the correlation time does not keep fixed the amplitude of the exponential term in equation 3.4. However, this choice allows us to fix the variance of the spike count in a long time window for each individual spike train while varying the timescale of its correlations. To make this clearer, consider the total number of presynaptic spikes arriving from the spike train i of the population p during a time window T, which is written as

$$N(T) = \int_0^T dt \sum_k \delta\left(t - t_i^k\right). \tag{3.5}$$

Notice that since the arrival times t_i^k are random in such a way that the train has the autocorrelation of equation 3.4, the number $N(T)$ is a random variable. Its mean value is

$$\langle N_p(T) \rangle = \left\langle \int_0^T dt \sum_k \delta\left(t - t_i^k\right) \right\rangle = \nu_p T, \tag{3.6}$$

___

[2]For renewal spike trains, the Fano factors in equation 3.4 are related to the coefficients of variation of their interspike intervals, CV_p, as $F_p = CV_p^2$. Note nevertheless that our formalism does not require that afferent spike trains are renewal.
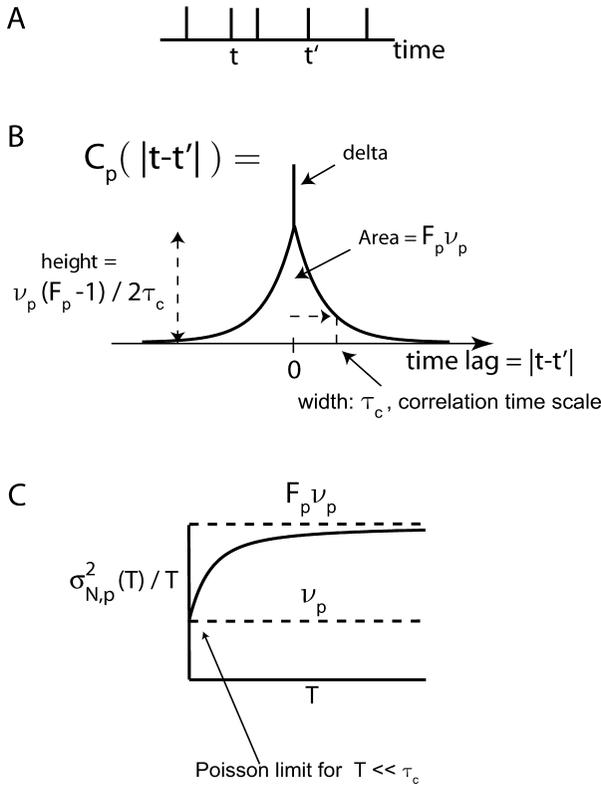
AUTO-CORRELATION FUNCTION

Figure 2: (A) An individual afferent spike train from population p could show correlations between two times, t and t': the probability of finding a spike at one of those times depends on the existence of a spike at the other time. (B) This temporal correlation is described by the autocorrelation function, $C_p(t - t')$, assumed to have an exponential shape. The firing rate, ν_p, Fano factor, F_p, and correlation time, τ_c, enter in the definition of the shape and size of the exponential as described in the plot. The delta function present at zero time is proportional to ν_p and participates in the total area of the autocorrelogram. (C) When the spike count of the spike train is integrated over a time window T, the variance of the count divided by T goes exponentially from ν_p to $F_{N,p}\nu_p$. For small time windows, the count variance converges to that of a Poisson spike train, which is equal to $\nu_p T$. However, for longer time windows than the correlation time τ_c, the count variance scales as $F_{N,p}\nu_p$, indicating that the effect of temporal correlations is then fully visible.

and its variance can be calculated using the autocorrelation defined in equation 3.4 as (Renart, Moreno-Bote, Wang, & Parga, 2007)

$$\sigma_{N,p}^2(T) = \left\langle \int_0^T dt \int_0^T dt' \sum_{k,k'} \delta\left(t - t_i^k\right) \delta\left(t' - t_i^{k'}\right) \right\rangle - \langle N_p(T) \rangle^2$$

$$= \int_0^T dt \int_0^T dt\, C_p(t, t')$$

$$= \nu_p T + \nu_p (F_p - 1)(T - \tau_c(1 - e^{-T/\tau_c})). \qquad (3.7)$$

Therefore, the variance of the spike count grows linearly with T for long windows $T \gg \tau_c$, where it takes the value

$$\sigma_{N,p}^2(T) = F_p \nu_p T \qquad (3.8)$$

(see Figure 2C). Thus, fixing only the Fano factor in the autocorrelation function keeps fixed the variance in the spike count for long T, as this variance is independent of τ_c. Changing τ_c does not alter the total spike count fluctuations, only the temporal precision in which they occur. Notice that the inclusion of the Fano factor in the autocorrelation function, equation 3.4, is consistent with its definition for long T in equation 3.1. Notice also from equation 3.7, that the variance of the spike count is $\nu_p T$ for short $T \ll \tau_c$, and therefore the afferent spike train looks like a Poisson spike train when it is sampled during brief time windows. However, as soon as T is comparable to the correlation time, the variance of the spike count starts to take into account the temporal correlations in the spike train, and when T becomes very large, all effects are included, and the variance is $F_p \nu_p T$, equation 3.8 (see Figure 2). We will show that for the LIF neuron we are considering, whether the input is seen as having significant temporal correlations depends on how the timescale of these correlations compares to the neuron's membrane time constant.

3.2 Cross-Correlograms. We have also considered the possibility that spikes in different trains are correlated. When the activity of two neighboring neurons is recorded, the cross-correlogram computed from their discharges can sometimes present a single peak with or without damped oscillations (e.g. Perkel, Gerstein, & Moore, 1967; Aersten, Gerstein, Habib, & Palm, 1989; deCharms & Merzenich, 1996). A prominent peak at zero time lag means that the two neurons tend to fire synchronously; if a dip is observed, when one neuron fires, the other is more likely to be silent. Very often the cross-correlograms can be approximated by an exponential function (e.g., deCharms & Merzenich, 1996; Bair et al., 2001). The cross-correlogram

is therefore modeled here as an exponential,

$$
\begin{aligned}
C_{pq}(t, t') &\equiv \left\langle \left(\sum_{k_p} \delta\left(t - t_i^{k_p}\right) - v_p \right) \left(\sum_{k_q} \delta\left(t' - t_j^{k_p}\right) - v_q \right) \right\rangle \\
&= \left\langle \sum_{k_p, k_q} \delta\left(t - t_i^{k_p}\right) \delta\left(t' - t_j^{k_q}\right) \right\rangle - v_p v_q \\
&= \sqrt{v_p v_q} \left(\frac{\rho_{pq} \sqrt{F_p F_q}}{2\tau_c} \right) e^{-\frac{|t - t'|}{\tau_c}},
\end{aligned}
\tag{3.9}
$$

where $C_{pq}(t, t')$ is the two-point correlation function between the trains (i, j) in populations p and q $(p, q = E, I)$. This cross-correlation function is illustrated in Figure 3B. As in the case of the autocorrelation defined in equation 3.4, the two-point correlation function expresses the probability density of finding a spike of a train in population p at time t along with a spike of a train in population q at time t', from which the probability density of finding them by chance, $v_p v_q$, is subtracted. The magnitude of the cross-correlations is determined by the correlation coefficients ρ_{pq} of the spike counts (see its definition in equation 3.11). For the sake of simplicity, we take all the correlations in the problem to have the same time constant τ_c.

To better understand the effects of cross-correlations on the input statistics, we calculate the covariance between the count of spikes emitted by the neuron i from population p and the count of spikes emitted by the neuron j from population q as an integral of the cross-correlation function, equation 3.9, as

$$
\begin{aligned}
\langle (N_p(T) - \langle N_p(T) \rangle)(N_q(T) - \langle N_q(T) \rangle) \rangle &= \langle N_p(T) N_q(T) \rangle - v_p v_q T^2 \\
&= \left\langle \int_0^T dt \int_0^T dt' \sum_{k_p, k_q} \delta\left(t - t_i^{k_p}\right) \delta\left(t' - t_j^{k_q}\right) \right\rangle - v_p v_q T^2 \\
&= \int_0^T dt \int_0^T dt' \, C_{pq}(t - t') \\
&= \sqrt{v_p v_q}(\rho_{pq} \sqrt{F_p F_q})(T - \tau_c(1 - e^{-T/\tau_c})).
\end{aligned}
\tag{3.10}
$$

This covariance measures the correlation in the spike count fluctuations during a time T from two presynaptic spike trains. Notice that for T much shorter than the correlation time, this covariance is zero, that is, the spike counts of the two neurons become independent. This is true because for short T, the spike trains look like uncorrelated Poisson trains. However, for time windows that are longer than the correlation time, the covariance is
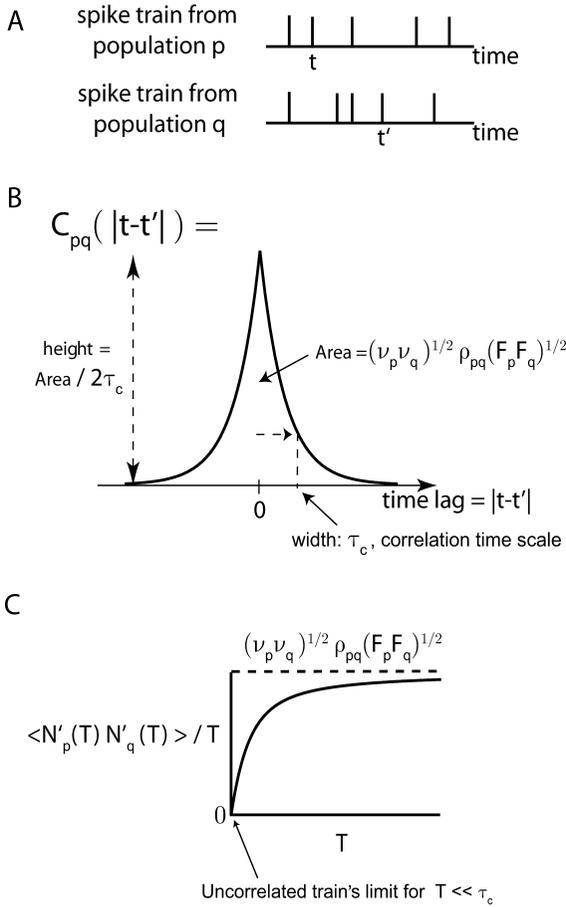
CROSS-CORRELATION FUNCTION

Figure 3: (A) The probability of having a spike at time t in an afferent spike train belonging to population p could depend on the existence of having a spike at time t' on another spike train from population q. (B). This correlation is described by the cross-correlation function, $C_{pq}(t - t')$, assumed to have exponential shape. The firing rates, Fano factors, correlation coefficient of the spike counts, ρ_{pq}, and correlation time, τ_c, determine the shape of the exponential, as illustrated in the figure. (C) When the spike counts of the spike trains in the top panel are integrated over a time window T, their covariance divided by T increases exponentially from zero to a finite value proportional to the correlation coefficient (here we define $N'(T) = N(T) - \langle N(T) \rangle$). For short time windows, the covariance is zero, and therefore it resembles that of two independent spike trains. However, for time windows longer than τ_c, correlations are fully visible, and the covariance is nonzero.

nonzero and approaches a linear behavior. This covariance as a function of the integration window is represented in Figure 3C.

The correlation coefficient is defined as the ratio of the covariance and the product of the deviations in the spike counts of both neurons, as

$$\rho_{pq} = \frac{\langle (N_p(T) - \langle N_p(T) \rangle)(N_q(T) - \langle N_q(T) \rangle) \rangle}{\sigma_{N_p}(T)\sigma_{N_q}(T)} \tag{3.11}$$

for long T. Notice from equation 3.10 that the inclusion of the correlation coefficient in the cross-correlation, equation 3.9, is consistent with the above definition. Changing the correlation time in the cross-correlation, equation 3.9, changes its amplitude but not the correlation coefficient between the two spike trains. The Fano factors appear in equation 3.9 because the time integral of the cross-correlation has to be zero if one of the trains does not have spike count fluctuations ($F_N = 0$).

3.3 Writing the Statistical Properties of the Total Current. The two-point correlation function of the total afferent current, equation 2.2, is defined as

$$C_{current}(t, t') \equiv \langle (I(t) - \langle I(t) \rangle)(I(t') - \langle I(t') \rangle) \rangle, \tag{3.12}$$

where the mean current $\langle I(t) \rangle$ is calculated as in equation 2.3. The correlation function should take into account both the auto- and cross-correlations of the spike trains in the E and I populations given in equations 3.4 and 3.9. In Figure 4 we depict a diagram with the correlations present in the E and I neurons, whose spikes trains impinge on the same target neuron. There are N_E excitatory neurons firing at rate ν_E and N_I inhibitory neurons with rate ν_I. We assume that only a fraction f_{EE} (f_{II}) of the N_E (N_I) excitatory (inhibitory) neurons are correlated with other neurons within the same population, with a correlation coefficient ρ_{EE} (ρ_{II}). Also only a fraction f_{EI} of the excitatory neurons are correlated with a fraction f_{EI} of the inhibitory neurons, with a correlation coefficient $\rho_{EI} = \rho_{IE}$.

Then the correlation function of the current, equation 3.12, contains several contributions:

$$\begin{aligned}
C_{current}(t, t') = {} & J_E^2 \, N_E \, C_E(t - t') + J_I^2 \, N_I \, C_I(t - t') \\
& + J_E^2 \, f_{EE} \, N_E \, (f_{EE}N_E - 1) \, C_{EE}(t - t') \\
& + J_I^2 \, f_{II} \, N_I \, (f_{II}N_I - 1) \, C_{II}(t - t') \\
& - 2 \, J_E \, J_I \, f_{EI} \, f_{IE} \, N_E \, N_I \, C_{EI}(t - t').
\end{aligned} \tag{3.13}$$

In this expression, the two first terms come from the autocorrelations of the spike trains in the E and I populations. The third and fourth terms
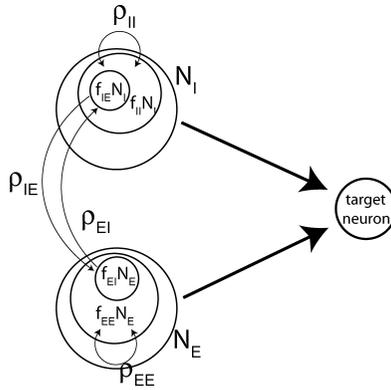
Figure 4: Diagram of correlations in excitatory (E) and inhibitory (I) neuronal populations presynaptic to the same target neuron. The presynaptic E and I populations make N_E and N_I contacts, respectively, with the target neuron. A fraction $f_{EE(II)}$ of these $N_{E(I)}$ excitatory (inhibitory) neurons are correlated with each other with a correlation coefficient $\rho_{EE(II)}$. Also there are $E - I$ correlations, with a fraction f_{EI} participating from the E population and a fraction f_{IE} from the I population, for which the correlation coefficient is ρ_{EI} ($=\rho_{IE}$). Since all E neurons in the fraction f_{EI} are correlated with any given I neuron in the fraction f_{IE}, these E neurons necessarily have $E - E$ correlations. Therefore, they are considered here to be a group within the fraction f_{EE}, as shown in the figure. The same applies for the I neurons.

take into account the cross-correlation between spike trains in the same E or I population. They are positive because both E and I inputs contribute positively to enhance fluctuations. The last term incorporates the cross-correlation between spike trains, one from the E population and the other from the I neuronal population, and it is negative. Indeed, positive correlations between E and I neurons always reduce synaptic fluctuations because the arrival of an excitatory spike can be cancelled out by the arrival of another inhibitory spike, and this happens with higher-than-chance probability. Therefore, the effect of correlations within E or I neurons is always to increase $C_{current}(t, t')$ in the direction of their cross-correlation functions, $C_{EE}(t - t')$ and $C_{II}(t - t')$, whereas the effect of correlations between E and I spike trains is always to lower the current correlation function in an amount proportional to $C_{EI}(t - t')$.

Using the choices given in equations 3.4 and 3.9, the two-point correlation function of the total input current to the neuron can be written as

$$C_{current}(t, t') = \sigma_w^2 \left[\delta(t - t') + \frac{\alpha}{2\tau_c} e^{-\frac{|t-t'|}{\tau_c}} \right], \tag{3.14}$$

where we call σ_w^2 the white noise variance, and α the correlation magnitude. They are expressed in terms of the model parameters as

$$\sigma_w^2 = J_E^2 \ N_E \ \nu_E + J_I^2 \ N_I \ \nu_I$$

$$\alpha \ \sigma_w^2 = J_E^2 \ \nu_E \ [(F_E - 1) + f_{EE} \ (f_{EE} \ N_E - 1) \ F_E \ \rho_{EE}]$$

$$+ J_I^2 \ N_I \ \nu_I \ [(F_I - 1) + f_{II} \ (f_{II} \ N_I - 1) \ F_I \ \rho_{II}]$$

$$- 2 \ J_E \ J_I \ f_{EI} \ f_{IE} \ N_E \ N_I \ \sqrt{\nu_E \ \nu_I} \ \sqrt{F_E \ F_I} \ \rho_{EI}. \tag{3.15}$$

We define the total variance of the current, σ_{eff}^2, as the sum of the white noise variance and the variance generated by correlations, $\alpha\sigma_w^2$, that is,

$$\sigma_{eff}^2 = \sigma_w^2(1 + \alpha). \tag{3.16}$$

The sign of the correlation magnitude determines the sign of the correlations. If $\alpha > 0$, the current has positive correlations, while if $\alpha < 0$, the current has negative correlations. The minimum physically possible value for the correlation magnitude is $\alpha = -1$.[3] If $\alpha = 0$, the current is uncorrelated. Notice that σ_{eff}^2 is very sensitive to the fractions of correlated input trains, as these fractions are multiplied by the number of connections from each population to the square, which typically are of the order of $10^3 - 10^4$. Also, from equation 3.15, it is possible to see that increasing the correlations between excitatory or inhibitory neurons (either increasing ρ_{EE} or ρ_{II}) enhances the total variance, whereas correlations between excitatory-inhibitory pairs (ρ_{EI}) always decrease it (Salinas & Sejnowski, 2000).

The parameters τ_c and α that appear in the definition of the correlation function of the current, equation 3.14, fully characterize both the temporal range and the intensity of the correlations relative to the white noise variance σ_w^2. Although it is important to understand the effect of these two parameters on the neuronal firing response separately, previous studies have not studied this problem. For instance, in Feng and Brown (2000), only the case $\tau_c = 0$ is considered, which precludes the characterization

---

[3]For large enough T ($T \gg \tau_c$), the variance of the integrated current, or accumulated charge $Q(t) = \int_0^T dt \, I(t)$, is calculated as

$$\text{Var}[Q(T)] = \int_0^T dt \int_0^T dt' \ C_{current}(t, t') = \sigma_{eff}^2 T.$$

Therefore, the variance of the current is just the proportionality factor σ_{eff}^2. Notice that since the variance of the current is nonnegative, the correlation magnitude has a lower bound at $\alpha = -1$. Lower values are not physically possible because the variance of a real-valued stochastic variable cannot be negative.

of the temporal scale of the correlations. On the other hand, Salinas and Sejnowski (2000) have changed simultaneously the values of τ_c and α in their simulations.

3.4 The Sum of a Large Number of Independent Non-Poisson Spike Trains Is Not Poisson. One point deserves clarification at this moment. It refers to the way many simultaneous spike trains add up. The sum of many independent spike trains has been commonly approximated as a Poisson process (e.g., Daley & Vere-Jones, 1988; Amit & Brunel, 1997a). Although this is in some cases a good approximation, it is worth emphasizing that the sum of many independent point processes is not, in general, Poisson. Indeed, the conditions for the sum process to be truly Poisson are rather restricted (see, e.g., Daley & Vere-Jones, 1988). In particular, one of the conditions implies that on any time interval, only one event can be observed from each individual point process. However, this is expected to be a good approximation only for time windows much shorter than the typical interspike interval of each neuron. In general, a neuron will receive one, two, or more spikes from the same presynaptic neuron before it fires, not just at most one spike, as the Poisson approximation strictly requires.

As expected from the rules of probability, adding up many independent spike trains results in a global spike train with an autocorrelation function with exactly the same functional form as those of the individual trains (note, however, that higher-order properties are not necessarily conserved, that is, the sum of many renewal processes may not be renewal). In particular, when N independent spike trains with an autocorrelation $C(t, t')$ are added, the summed train has an autocorrelation $N \times C(t, t')$ (Moreno et al., 2002; see also equation 3.13 with $C_{EE(II,EI)} = 0$ and $J_{E(I)} = 1$). We further noted that even in the diffusion limit ($N \to \infty$), when the individual firing rates ν are renormalized by ν/N to yield a finite two-point correlation function, the autocorrelation function of the total input has exactly the same shape as the autocorrelation function of the individual spike trains. Later works have also used this property (Renart et al., 2007; Lindner, 2006; Cateau & Reyes, 2006; Doiron, Rinzel, & Reyes, 2006), which is relevant to describe the temporal aspects of correlations in networks of spiking neurons.

Here we exemplify the above result using the expression for the correlation function of the current, equations, 3.14 and 3.15. It is easy to see that the total current will show temporal correlations beyond the trivial delta function at zero time lag whenever α is different from zero and τ_c is not infinity. If the afferent spike trains are independent ($\rho = 0$) but they have exponential autocorrelations, like those in equation 3.4, then α will be different from zero (see equation 3.15). This will happen for any choice of the number of connections and synaptic strengths (different from zero). Therefore, no matter which choices of the parameters are taken, the correlation function of the total current can never correspond to a Poisson process with a larger rate, since an input Poisson process will produce a correlation

function equal to $C_{current}(t, t') = \sigma_w^2 \delta(t - t')$. The above argument does not depend on the condition that the correlations are exponential, but rather the same conclusion can be achieved from equation 3.13 using any plausible autocorrelation function $C_E(t, t')$ and $C_I(t, t')$ different from a delta function (i.e., different from the autocorrelation function of a Poisson process).

3.5 When the Current Can Be Approximated by a Gaussian Current.
We have described the statistical properties of the total current, $I(t)$, generated by correlated spike trains. However, the firing response of a neuron receiving that current is not yet completely determined by the mean and two-point correlation function of the current alone, equations 3.14 and 3.15. These quantities describe the statistical properties of a stationary current up to second order, but higher-order statistics in the input could also play a role in shaping the firing response of the neuron. However, if the current $I(t)$ can be approximated by a gaussian process, then the current would be fully described by its mean and two-point correlation function. In fact, gaussianity naturally holds when the neuron is receiving a large barrage of uncorrelated spikes per second, each one inducing a membrane depolarization J very small compared to the distance between the threshold and reset potentials, $J/(\Theta - H) \ll 1$ (Ricciardi, 1977). When inputs are correlated, the net effect of correlations is to increase effectively the size of the unitary depolarization (for positive correlations), since two or more spikes are more likely to occur together in time. We have estimated this renormalization in the size of J and determine that for the gaussian approximation to be valid with correlated input spike trains, the condition

$$\frac{J F}{(\Theta - H)}(1 + f N \rho) \ll 1 \tag{3.17}$$

should hold. This is a heuristic formula, and it is explained qualitatively as follows. The worst condition in the presence of correlations occurs when the correlation time τ_c is zero, that is, when there is some chance that two or more spikes arrive at the same time, increasing the effective size of each spike and worsening the gaussian approximation. One can estimate the mean number of spikes arriving together to be $F(1 + f N \rho)$, which grows with the variability of the spike trains, the number of correlated pairs, and their correlation coefficient. As long as this number multiplied by J is small compared to $\Theta - H$, equation 3.17, the gaussian approximation is expected to be appropriate. This indicates that if either F, fN, or ρ increases too much, the gaussian limit will be broken. When condition 3.17 is largely broken, as in Kuhn, Aertsen, and Rotter (2003), the gaussian approximation is no longer valid. In particular, in the limit of large N, it should hold that $\rho \sim 1/fN$, so the correlation coefficients cannot remain finite as the size of the population of neurons with significant cross-correlations increases.

If condition 3.17 is satisfied, the input current in our problem can be described as a gaussian stochastic current fully defined in terms of the mean $\mu = J_E N_E \nu_E - J_I N_I \nu_I$, the variance σ_w^2, the correlation magnitude (α) and correlation time (τ_c), as expressed in equation 3.14.

3.6 Choosing the Connectivity and Correlation Parameters. Because we are dealing with a model with many free parameters (see equation 3.15), here we fix most of them or make choices within a range of realistic values. A single neuron receives typically $N_E \sim 5000 - 60000$ excitatory connections from other neurons (Cragg, 1967; DeFelipe & Fariñas, 1992). This accounts for 80% of the total number of synapses; the remaining 20% corresponds to inhibitory synapses (Abeles, 1991). The dynamical range of cortical neurons lies in the interval $\nu \sim 0 - 200$ Hz (Albright, 1993), although lower rates are much more probable than higher ones (Rolls & Treves, 1998). Synaptic strengths are between $J = 0.1 - 1$ mV (Amit & Brunel, 1997a; see the references there). Assuming a threshold of 20 mV above the resting potential of the neuron, these unitary events represent a fraction in the range $J \sim 5 \, 10^{-3} - 10^{-2}$ of the total path to be traveled from rest to firing threshold.

Fano factors of the spike count lying in the interval 1 to 1.5 reveal higher irregularity in the neuronal discharges from that expected from Poisson trains (Dean, 1981; Softky & Koch, 1993; Shadlen & Newsome, 1998; Albright, 1993; Stevens & Zador, 1998; Compte et al., 2003).

The timescale of correlations varies from a few to several hundred milliseconds, $\tau_c \sim 1 - 100$ ms (Ts'o, Gilbert, & Wiesel, 1986; Gochin, Miller, Gross, & Gerstein, 1991). For instance, in deCharms and Merzenich (1996) the correlated activity of pairs of neurons in primary auditory cortex in cats was recorded. The mean half-width at half-height of the cross-correlograms peaks computed from these pairs was ∼10 ms, which corresponds to a correlation timescale $\tau_c = 10 \text{ ms}/\ln 2 \sim 15$ ms.

Zohary et al. (1994) have reported correlation coefficients of $\rho = 0.12$ between neighboring cells in the middle temporal visual area (MT, or V5). If any pair of neurons in a group of thousand units were correlated with such a magnitude and projected to a same target neuron, the magnitude of the input fluctuations would be unrealistically large (see equation 3.15). In fact, the value $\rho = 0.12$ holds only for units within local circuits, because it is known that more distant neurons display much smaller correlation coefficients (Lee et al., 1998). Although a "mean" correlation coefficient could have been considered,[4] we have taken into account the heterogeneity of pairwise correlations observed in the cortex by assuming that only a fraction f_{pq} of neurons between populations p and q are indeed

---

[4]A mean correlation coefficient can be obtained by averaging the ρ of each pair of neurons: $\langle \rho \rangle = \int f(\rho) d\rho$.

correlated with the same correlation coefficient ρ_{pq}. This fraction could represent the portion of presynaptic neurons located in the surroundings of the target neuron, and thus embedded in the same local circuits as this neuron, or a far neuronal population displaying correlations between its units and projecting to the same target neuron. To bound the effects of input correlations, we assume that around 1% of the presynaptic neurons can be correlated. Such a small value of f_{pq} still produces a large effect on the correlation magnitude (see equation 3.15), as will also be clear in section 7.2.

The values of μ, σ_w^2, and α therefore lie within rather broad intervals. As an example of the typical values they can take, if a neuron receives $N_E = 10^4$ excitatory connections, $N_I = 2 \, 10^3$ inhibitory connections, with synaptic strengths $J_E = 5 \, 10^{-3}$ and $J_I = 2 \, 10^{-2}$ (in units of the threshold), and they are firing at $\nu_E = \nu_I = 5$ Hz, then $\mu = 50$ Hz and $\sigma_w^2 = 5.3$ Hz. Assuming that there are correlations only between pairs of neurons in the E population ($\rho_{EI} = \rho_{II} = 0$), being $f_{EE} = 0.1$ the fraction of those that are correlated, then $\alpha = 0.85$ if $F_E = F_I = 1.5$ and the correlation coefficient is $\rho_{EE} = 0.01$, or $\alpha = 4$ if $\rho_{EE} = 0.1$. When we present results from numerical simulations, the parameter values considered will be of the order of the ones mentioned above.

4 Two Ways of Transforming the Non-Markovian Problem into a Markovian One

As we explained in section 1, we aim at calculating the output firing rate of an LIF neuron receiving a correlated input as described in the previous sections. The main technical problem in studying the response properties of a neuron driven by correlated inputs analytically is that the stochastic process defined by equation 2.1 with a current having correlations as in equation 3.14 is non-Markovian, that is, the time derivative of the membrane potential at each time depends on the past history of the afferent current, not only on its present value. This fact complicates the solution of the problem. However, the process defined in equations 2.1 and 3.14 can be expressed in a Markovian way by generating the current $I(t)$ with the help of an Ornstein-Uhlenbeck process (Moreno et al., 2002). The stochastic current $I(t)$ generated in this way displays exactly the same exponential correlations as equation 3.14. This duplicates the number of variables but puts the problem in a suitable form (see equations 4.1 and 4.2 and 4.11 and 4.12 below). We have found two different ways of representing the correlated gaussian current $I(t)$ satisfying equation 3.14. They differ only in the values of α for which they hold. While one of them is more general because α can take any physical value (including both positive and negative correlations), the other is simpler, although it can be used only for $\alpha > 0$ (positive correlations).

4.1 The First Representation for the Dynamics of $I(t)$. The first representation of the current $I(t)$ that we discuss here generates both positive ($\alpha > 0$) and negative ($\alpha < 0$) correlations. It has the form

$$I(t) = \mu + \sigma_w \eta(t) + \sigma_w \frac{\beta}{\sqrt{2\tau_c}} z(t) \tag{4.1}$$

$$\dot{z}(t) = -\frac{z}{\tau_c} + \sqrt{\frac{2}{\tau_c}} \eta(t), \tag{4.2}$$

where $\eta(t)$ is a white noise random process with mean zero and unit variance (i.e., $\langle \eta(t) \rangle = 0$ and $\langle \eta(t)\eta(t') \rangle = \delta(t - t')$), $\beta = \sqrt{1 + \alpha} - 1$, and $z(t)$ is an auxiliary colored random process that obeys the Ornstein-Uhlenbeck process, equation 4.2, with the same white noise $\eta(t)$ (see, e.g., Risken, 1989).

It is easy to check that the current defined in equations 4.1 and 4.2 generates a gaussian waveform with mean $\langle I(t) \rangle = \mu$ and exponential correlations as in equation 3.14. Defining $i(t) = (I(t) - \mu)/\sigma_w$, we have

$$\langle i(t)\, i(t') \rangle = \left\langle \left[\eta(t) + \frac{\beta}{\sqrt{2\tau_c}} z(t) \right] \left[\eta(t') + \frac{\beta}{\sqrt{2\tau_c}} z(t') \right] \right\rangle$$

$$= \delta(t - t') + \frac{\beta}{\sqrt{2\tau_c}} \langle \eta(t)z(t') \rangle + \frac{\beta}{\sqrt{2\tau_c}} \langle \eta(t')z(t) \rangle + \frac{\beta^2}{2\tau_c} \langle z(t)z(t') \rangle. \tag{4.3}$$

Assuming that $t' > t$ without loss of generality (because $\langle i(t)\, i(t') \rangle$ is symmetric in the steady state), the third term on the right side of equation 4.3 vanishes. The second and fourth terms are calculated using the solution of the stochastic equation, equation 4.2,

$$z(t) = \sqrt{\frac{2}{\tau_c}}\, e^{-t/\tau_c} \int_0^t ds\, e^{s/\tau_c}\, \eta(s), \tag{4.4}$$

with the initial condition $z(0) = 0$. We find that in the stationary state ($t, t' \to \infty$, $t' - t = $ constant > 0),

$$\langle \eta(t)z(t') \rangle = \sqrt{\frac{2}{\tau_c}}\, e^{-(t'-t)/\tau_c}$$

$$\langle z(t)z(t') \rangle = e^{-(t'-t)/\tau_c}.$$

When we use these identities, the correlation function of the current $I(t)$ defined in equations 4.1 and 4.2, denoted $C_{current}(t, t')$, can be written as

$$C_{current}(t, t') \equiv \langle (I(t) - \mu)(I(t') - \mu) \rangle$$

$$= \sigma_w^2 \left[\delta(t - t') + \frac{\beta(2 + \beta)}{2\tau_c}\, e^{-\frac{|t-t'|}{\tau_c}} \right], \tag{4.5}$$

from where one sees that the correlation magnitude α is related to the new parameter β by $\alpha = \beta(2 + \beta)$, an equation that has two independent solutions, $\beta = \pm\sqrt{1 + \alpha} - 1$, both equally valid. We have chosen $\beta = \sqrt{1 + \alpha} - 1$. Remember that α has a lower bound in -1, which is obtained with $\beta = -1$. For each solution there is a one-to-one mapping from $\alpha \in [-1, +\infty)$ to β, and thus all physically realizable positive and negative correlations are included in this formalism.

The joint process defined by equations 2.1, 4.1, and 4.2 is Markovian and driven by white noise. Thus, the problem of finding the output firing rate can be formulated according to its associated stationary Fokker-Planck equation (FPE) (Risken, 1989). The system of equations 2.1, 4.1, and 4.2 can be simplified by the linear transformation,

$$V = \mu\tau_m + \sigma_w\sqrt{\frac{\tau_m}{2}}x, \tag{4.6}$$

to obtain the set of stochastic equations:

$$\dot{x}(t) = -\frac{x(t)}{\tau_m} + \sqrt{\frac{2}{\tau_m}}\eta(t) + \frac{\beta}{\sqrt{\tau_m\tau_c}}z(t)$$

$$\dot{z}(t) = -\frac{z}{\tau_c} + \sqrt{\frac{2}{\tau_c}}\eta(t).$$

The FPE associated with these two equations is derived in detail in appendix B and is given by

$$\left[L_x + \frac{L_z}{k^2} + \frac{2}{k}\frac{\partial}{\partial x}\left(\frac{\partial}{\partial z} - \frac{\beta z}{2}\right)\right]P_\beta(x, z) = -\tau_m\delta(x - \sqrt{2}\hat{H})J_\beta(z),$$

$$\tag{4.7}$$

where the differential operator L_u is defined as $L_u = \frac{\partial}{\partial u}u + \frac{\partial^2}{\partial^2 u}$, and $k \equiv \sqrt{\tau_c/\tau_m}$. Besides, $\hat{H} = \frac{H - \mu\tau_m}{\sigma_w\sqrt{\tau_m}}$ and $\hat{\Theta} = \frac{\Theta - \mu\tau_m}{\sigma_w\sqrt{\tau_m}}$. The true reset and threshold values in the new variable x are $\sqrt{2}\hat{H}$ and $\sqrt{2}\hat{\Theta}$, respectively. The function $P_\beta(x, z)$ is the steady-state probability density of having the neuron in the state (x, z). Since the problem cannot be solved exactly as in the one-dimensional diffusion case (see, e.g., Ricciardi, 1977; Risken, 1989), we have used a perturbative expansion of the FPE in powers of $k^{-1} = \sqrt{\tau_m/\tau_c}$.

A key quantity is the escape probability density flux at fixed z, $J_\beta(z)$. Associated to the FPE, equation 4.7, there is a probability density vector flux $\vec{J}_\beta(x, z)$ defined at each point on the plane (x, z) (Risken, 1989, p. 133). It measures the direction and the intensity of the probability density flux at

each point (x, z). For our FPE, it has the expression

$$\vec{J}_\beta(x, z) = \frac{1}{\tau_m} \left[-\frac{\partial}{\partial x} - x - \frac{1}{k} \left(\frac{\partial}{\partial z} - \beta z \right), \right.$$
$$\left. -\frac{1}{k^2} \left(\frac{\partial}{\partial z} + z \right) - \frac{1}{k} \frac{\partial}{\partial x} \right] P_\beta(x, z). \tag{4.8}$$

The probability density flux satisfies the so-called continuity equation,

$$\vec{\nabla} \cdot \vec{J}_\beta(x, z) + \tau_m \delta(x - \sqrt{2}\hat{H}) J_\beta(z) = 0, \tag{4.9}$$

where $\vec{\nabla} = [\frac{\partial}{\partial x}, \frac{\partial}{\partial z}]$ is the divergence operator. Equation 4.9 is equivalent to the FPE, equation 4.7, and expresses the conservation of the total probability over time. The escape probability density flux $J_\beta(z)$ is just the x-component of the probability density flux, equation 4.8, evaluated at threshold:

$$J_\beta(z) = \frac{1}{\tau_m} \left(-\frac{\partial}{\partial x} - x - \frac{1}{k} \left(\frac{\partial}{\partial z} - \beta z \right) \right) P_\beta(x, z)|_{x=\sqrt{2}\Theta}. \tag{4.10}$$

The escape probability density flux appears in equation 4.7 as a source term representing the reset effect: whenever the potential V reaches the threshold Θ, it is reset to the value H with the same z distribution that it had when it escaped. This holds because the particular value of z at the moment of the generation of each spike has to be conserved for the next interspike interval since, as opposed to V, z is not reset after an action potential. Crucially, this self-consistency condition complicates the solution of the FPE, equation 4.7. The escape probability density flux in equation 4.10 is exact if $\tau_{ref} = 0$ (or approximately if $\tau_c \gg \tau_{ref}$, because in this case, the variable z has slow dynamics and therefore its probability distribution at a time τ_{ref} after the emission of an output spike is very similar to its distribution at the moment of the spike).

Let us notice that this first representation of $I(t)$ can be used not only for analytical calculations but also for the numerical generation of exponentially correlated currents, as it is shown in Figure 5, where we show the exponential two-point correlation function of a current $I(t)$ generated numerically by equations 4.1 and 4.2 and that predicted by equation 4.5. Additionally, in section 7, this representation will be employed in the numerical analysis of the response of LIF neuron to negative and positive correlations.

4.2 The Second Representation for the Dynamics of $I(t)$. An afferent current $I(t)$ with nonnegative exponential correlations obeying
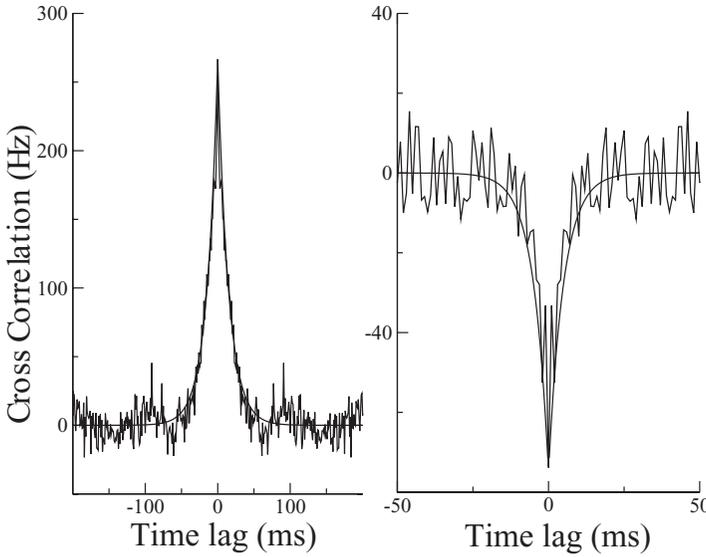
Figure 5: Normalized correlation functions of the current $I(t)$ numerically generated by simulating the process defined in equations 4.1 and 4.2. The normalized correlation function of the current is defined as $\hat{C}_{current}(s) = C_{current}(s)/\sigma_w^2 - \delta(s)$, where $C_{current}(s)$ is defined in equation 4.5. The variable s is the time lag $s = t - t'$. With this normalization, the correlation function has units of Hz. For positive correlations (left), we took $\beta = 2$, which yields a correlation magnitude $\alpha = 8$; $\tau_c = 15$ ms. For negative correlations (right) we took $\beta = -0.5$, which corresponds to $\alpha = -0.75$; here $\tau_c = 5$ ms. In both cases, numerical results are compared with the exponential functions predicted by equation 4.5 (nonfluctuating curves).

equation 3.14 can also be generated by the set of equations

$$I(t) = \mu + \sigma_w \eta(t) + \sigma_w \sqrt{\frac{\alpha}{2\tau_c}} y(t) \tag{4.11}$$

$$\dot{y}(t) = -\frac{y}{\tau_c} + \sqrt{\frac{2}{\tau_c}} \zeta(t). \tag{4.12}$$

Here $\eta(t)$ and $\zeta(t)$ are two independent white noise processes with mean zero and unit variance. The two-point correlation of $I(t)$ can be calculated as in equation 4.3, with the exceptions that β in equation 4.3 is replaced by $\sqrt{\alpha}$ and the two white noises are not correlated. Then only the terms analogous to the first and fourth terms in equation 4.3 are nonzero. Because

$\sqrt{\alpha}$ is a real number, the correlation magnitude α has to be positive in this representation.

From the set of equations 2.1, 4.11, and 4.12 making the linear transformation defined in equation 4.6, we obtain the FPE (the derivation is similar to the one presented in appendix B):

$$\left[L_x + \frac{L_y}{k^2} - \frac{\sqrt{\alpha} y}{k} \frac{\partial}{\partial x} \right] P_\alpha(x, y) = -\tau_m \delta(x - \sqrt{2} \hat{H}) J_\alpha(y). \qquad (4.13)$$

The linear differential operator L_u has been defined as in section 4.1, and again $k \equiv \sqrt{\tau_c / \tau_m}$. As in the previous representation, the escape probability density flux $J_\alpha(y)$ acts as a source term injecting current at the reset potential at the same rate and with the same distribution in y as when it escaped (here we have to assume that $\tau_{ref} = 0$, or $\tau_c \gg \tau_{ref} = 0$). It represents the probability current in the direction of x evaluated at threshold. The probability density vector flux for this FPE is

$$\vec{J}_\alpha(x, y) = \frac{1}{\tau_m} \left[-\frac{\partial}{\partial x} - x - \frac{\sqrt{\alpha} y}{k}, \quad -\frac{1}{k^2} \left(\frac{\partial}{\partial y} + y \right) \right] P_\alpha(x, y). \qquad (4.14)$$

Its continuity equation is

$$\vec{\nabla} . \vec{J}_\alpha(x, y) + \tau_m \delta(x - \sqrt{2} \hat{H}) J_\alpha(y) = 0, \qquad (4.15)$$

equivalent to the FPE, equation 4.13, and the escape probability density flux is defined as

$$J_\alpha(y) = \frac{1}{\tau_m} \left(-\frac{\partial}{\partial x} - x - \frac{\sqrt{\alpha} y}{k} \right) P_\alpha(x, y)|_{x=\sqrt{2} \hat{\Theta}}. \qquad (4.16)$$

The FPE, equation 4.13, will be useful for finding a perturbative solution to the first passage time problem in powers of $k = \sqrt{\tau_c / \tau_m}$, that is, for short, τ_c. We have found this representation especially useful for this purpose, since this limit is harder to obtain from the first representation.

4.3 Conditions over the Probability Density Distribution and Probability Density Flux. For both representations of exponential correlations, the probability density and the escape probability density flux must be determined such that they obey the set of conditions:

1. Normalization of the probability density,

$$\tau_{ref} \nu_{out} + \int_{-\infty}^{\sqrt{2} \hat{\Theta}} dx \int_{-\infty}^{\infty} dw \, P_r(x, w) = 1 \qquad (4.17)$$

2. Threshold vanishing condition,

$$P_r(\sqrt{2}\hat{\Theta}, w) = 0 \tag{4.18}$$

3. The output firing rate is given by

$$\nu_{out} = \int_{-\infty}^{\infty} dw \, J_r(w). \tag{4.19}$$

4. The escape probability density flux has the form

$$J_r(w) = -\frac{1}{\tau_m} \frac{\partial}{\partial x} P_r(x, w)|_{x=\sqrt{2}\hat{\Theta}} \tag{4.20}$$

where $r = \alpha, \beta$ is the representation label, and w stands for both z and y.

Condition 4.17 is a normalization condition stating that with probability $\tau_{ref}\nu_{out}$, the neuron is in the refractory period. Condition 4.18 states that at the firing threshold, the probability density has to be zero (notice that the density can be defined to be zero above threshold, so this condition is a continuity condition at the threshold boundary). This is so because otherwise, the flux in equation 4.20, which includes a derivative evaluated at threshold, would be infinity. The output firing rate of the neuron, ν_{out}, is obtained by integrating the escape probability density flux over w, condition 4.19. To write down $J_r(w)$ in condition 4.20, we have used condition 4.18 applied to equations 4.10 and 4.16. Notice that precisely because of condition 4.18, the escape probability density flux, equation 4.20, has exactly the same expression in both representations.

While solving the FPEs in both representations, it is usually easier to employ the exact condition,

$$\int_{-\infty}^{\sqrt{2}\hat{\Theta}} dx \, P_r(x, w) = (1 - \nu_{out}\tau_{ref}) \frac{e^{-w^2/2}}{\sqrt{2\pi}} \, , \tag{4.21}$$

which is directly obtained from the equations for z or y (see equations 4.2 and 4.12, respectively) and the condition that there is a fraction $\nu_{out}\tau_{ref}$ of neurons in the refractory state. Equation 4.21 states that the marginal distribution of w is a normal distribution, as it corresponds to the stationary distribution of an Ornstein-Uhlenbeck process (see equations 4.2 and 4.12). Notice that it is consistent with equation 4.17.

5 Output Firing Rate for Long and Short τ_c

The next step is to compute the output firing rate using the FPEs. We found it feasible to evaluate it from the first representation, equation 4.7, for long correlation times ($\tau_c \gg \tau_m$) and from the second representation, equation 4.13, for both short and long correlation times. In the two cases, we propose a perturbative expansion of the solution $P_r(x, w)$ in powers

of a representative temporal scale parameter (a convenient power of $k \equiv \sqrt{\tau_c/\tau_m}$).

5.1 Long τ_c Limit Using the First Representation. In this limit, we expand both the probability density and the escape probability density flux as a series in powers of $k^{-1} = \sqrt{\tau_m/\tau_c}$,

$$P_\beta(x, z) = h_0(x, z) + k^{-1}h_1(x, z) + k^{-2}h_2(x, z) + O(k^{-3}) \tag{5.1}$$

$$J_\beta(z) = J_{0,\beta}(z) + k^{-1}J_{1,\beta}(z) + k^{-2}J_{2,\beta}(z) + O(k^{-3}). \tag{5.2}$$

Each term $J_{i,\beta}$ in this expansion must satisfy condition 4.20,

$$J_{i,\beta}(z) = -\frac{1}{\tau_m}\frac{\partial}{\partial x}h_i(x, z)|_{x=\sqrt{2}\Theta}. \tag{5.3}$$

Let us proceed to the calculation by replacing the expansions 5.1 and 5.2 into the FPE, equation 4.7. This substitution generates a set of equations for $P_{i,\beta}$ that can be solved consistently with conditions 4.17 to 4.19. The main steps of the procedure are given in appendix C.

The resulting escape probability density flux $J_\beta(z)$ is found to be, up to $O(k^{-2})$,

$$J_\beta(z) = \frac{e^{-z^2/2}}{\sqrt{2\pi}}\left[v_0 + \sqrt{\frac{\tau_m^3}{\tau_c}\frac{(2+\beta)v_0^2(R(\hat{\Theta}) - R(\hat{H}))}{1 - v_0\tau_{ref}}}z\right.$$

$$\left. + \frac{\alpha}{\tau_c}C + \frac{\alpha C}{\beta^2\tau_c(1 - v_0\tau_{ref})}(z^2 - 1)\right],$$

$$C \equiv \tau_m^2 v_0^2\left[\frac{\tau_m v_0(R(\hat{\Theta}) - R(\hat{H}))^2}{1 - v_0\tau_{ref}} - \frac{\hat{\Theta}R(\hat{\Theta}) - \hat{H}R(\hat{H})}{\sqrt{2}}\right].$$

Here $R(t) = \sqrt{\frac{\pi}{2}}e^{t^2}(1 + \mathrm{erf}(t))$, where $\mathrm{erf}(t) = \frac{2}{\sqrt{\pi}}\int_0^t du\, e^{-u^2}$ is the error function. The rate v_0 is just the firing rate of a LIF neuron driven by a white noise input with variance σ_w^2 (Ricciardi, 1977),

$$v_0^{-1} = \tau_{ref} + \sqrt{\pi}\tau_m\int_{\hat{H}}^{\hat{\Theta}} dt\, e^{t^2}(1 + \mathrm{erf}(t)). \tag{5.4}$$

Notice that C is independent of τ_c.

We then use condition 4.19 to find the output firing rate valid for long τ_c and fixed α,

$$\nu_{out} = \nu_0 + \frac{\alpha}{\tau_c} C \ . \tag{5.5}$$

Several important conclusions can be extracted from this simple expression. First, the effect of correlations is linear on α for long τ_c. That is, doubling α doubles the firing rate above the rate without correlations, ν_0. Notice also that α can be positive or negative, so for negative correlations, the effect on the rate is the opposite of that for positive correlations. Second, the firing rate of an LIF neuron with exponentially correlated input approaches the firing rate in the absence of input correlations as the correlation time increases. This happens because as the correlation time becomes longer than the membrane time constant ($\tau_c \gg \tau_m$), the neuron filters out the fluctuations provoked by input correlations. As a consequence, in the long τ_c limit and for finite correlation magnitude, the correlated input to the neuron can be approximated by a white noise process. Therefore, in this limit, the observation of only the output firing rate of the neuron does not allow distinguishing a correlated input from one generated by the sum of many Poisson point processes in the diffusion limit. This result is important, as it determines when inputs with complex correlation structure (i.e., with several correlation timescales) can be approximated by white noise.

5.2 Long τ_c Limit using the Second Representation. In this section we calculate the firing rate in the long τ_c limit using the FPE, equation 4.13. Although the FPE in equation 4.13 is more restrictive than the FPE in equation 4.7 (it describes only positive correlations, $\alpha > 0$), it is analyzed here because it is much simpler and can also be solved in the limit in which α/τ_c is constant, that is, for arbitrarily large α. In fact, the FPE, equation 4.7, has been studied in the limit in which α/τ_c approaches zero as τ_c rises, because the correlation magnitude was constant in that case. The real advantage of using the second representation is that the predicted firing rate is valid for larger values of α, compared to formula 5.5.

We start from the FPE, equation 4.13, and assume that the factor $\sqrt{\alpha}/k$ is constant ($k \equiv \sqrt{\tau_c/\tau_m}$). We thus define

$$\gamma = \frac{\sqrt{\alpha}}{k}. \tag{5.6}$$

Inserting this parameter in equation 4.13, we obtain

$$\left[L_x - \gamma y \frac{\partial}{\partial x} + \frac{L_y}{k^2} \right] P_\alpha(x, y) = -\tau_m \delta(x - \sqrt{2}\hat{H}) J_\alpha(y), \tag{5.7}$$

where $J_\alpha(y)$ reads as in equation 4.20. The solution of the FPE, equation 5.7, along with conditions 4.17 to 4.21 in the long τ_c limit is found by expanding $P_\alpha(x, y)$ and the escape probability density flux $J_\alpha(y)$ in powers of k^{-2} while keeping γ fixed as

$$P_\alpha(x, y) = r_0(x, y) + k^{-2} r_1(x, y) + O(k^{-4})$$

$$J_\alpha(y) = J_{\alpha,0}(y) + k^{-2} J_{\alpha,1}(y) + O(k^{-4}). \tag{5.8}$$

To obtain the coefficients $r_i(x, y)$ and $J_{\alpha,i}(y)$ we proceed as in section 5.1. In particular, conditions 4.17 to 4.20 are imposed order by order. The main steps of the calculation are given in appendix D. The results are here summarized up to order k^0. The density $P_\alpha(x, y)$ up to $O(k^0)$ is

$$P_\alpha(x, y) = \tau_m J_\alpha(y) \, e^{-\frac{(x-\gamma y)^2}{2}} \int_x^{\sqrt{2}\hat{\Theta}} du \, e^{\frac{(u-\gamma y)^2}{2}} \, \mathcal{H}(u - \sqrt{2}\hat{H}), \tag{5.9}$$

($\mathcal{H}(t) = 1$ if $t > 0$ and it is zero otherwise), where the escape probability density flux $J_\alpha(y)$ up to the same order is

$$J_\alpha(y) = \frac{1}{\sqrt{2\pi}\,\tau_m} \, e^{-\frac{y^2}{2}} \left[\int_{\sqrt{2}\hat{H}-\gamma y}^{\sqrt{2}\hat{\Theta}-\gamma y} du \, e^{\frac{u^2}{2}} \int_{-\infty}^u dv \, e^{-\frac{v^2}{2}} \right]^{-1}. \tag{5.10}$$

The output firing rate at leading order is obtained by integrating $J_\alpha(y)$ over y as

$$\nu_{out} = \frac{1}{\sqrt{2\pi}\,\tau_m} \int_{-\infty}^{\infty} dy \, e^{-\frac{y^2}{2}} \left[\int_{\sqrt{2}\hat{H}-\gamma y}^{\sqrt{2}\hat{\Theta}-\gamma y} du \, e^{\frac{u^2}{2}} \int_{-\infty}^u dv \, e^{-\frac{v^2}{2}} \right]^{-1}. \tag{5.11}$$

Notice that this formula has been derived for $\tau_{ref} = 0$. Notice also that only the leading order k^0 has been calculated. This order, however, gives a firing rate that is much more accurate than the firing rate obtained using the first representation in the same limit, equation 5.5. This is true because the firing rate in equation 5.11 depends on γ, which is a function of the parameters α and k ($\gamma \equiv \sqrt{\alpha}/k$). If the zeroth-order firing rate in equation 5.11 is expanded in powers of k^{-1} for fixed α, the same firing rate in equation 5.5 is found when correlations are positive. (In particular, if $\alpha = 0$, then $\gamma = 0$ and ν_{out} equals ν_0, that is, the well-known expression for the firing rate of an LIF neuron driven by white noise; Ricciardi, 1977.) This means that equation 5.11 is exact up to $O(k^{-2})$, and therefore the corrections to the firing rate arising from the terms $O(k^{-2})$ in the expansion 5.8 should vanish. This is indeed the case, as shown in appendix D. In addition, the higher-order corrections found in the expansion of equation 5.11 improve the prediction

provided by equation 5.5, especially when α is very large or when α/τ_c is kept constant (i.e., γ constant) in the long τ_c limit.

The firing rate in equation 5.11 has a very simple interpretation. Since y is slow compared to the voltage dynamics ($\tau_c > \tau_m$), the firing rate of an LIF neuron receiving correlated noise can be calculated by multiplying the firing rate of the LIF neuron receiving a frozen current proportional to y (plus mean μ and white noise with amplitude σ_w; this corresponds to the function into the square brackets, divided by τ_m; Ricciardi, 1977)[5] and the probability density of having the value y, which in this case is a normal distribution because y obeys an Ornstein-Uhlenbeck process, equation 4.12. This expression, obtained here to describe the effect of exponentially correlated inputs, has also been used to describe the effects of synaptic filtering with both fast and slow linear synapses on the output firing rate of an LIF neuron (Moreno-Bote & Parga, 2004).

One important feature of the firing rate in the long τ_c limit, equation 5.11, is that it does not change as γ is kept fixed, that is, as the ratio α/τ_c is kept constant. This means that to obtain the same output firing rate for a longer correlation time, one has to increase proportionally the correlation magnitude so that the loss of temporal precision is counterbalanced by an increase in the excess of synchronous afferent spikes. This suggests a proportionality law that could be tested experimentally using in vitro current injections in which both the magnitude and the temporal precision can be controlled independently (using, e.g., equation 4.2). Furthermore, for nonexponential correlation functions (e.g., oscillatory), it might be possible to define an effective correlation magnitude and an effective correlation time so that the output firing rate of the neuron will not depend on them individually but on their ratio.

5.3 Short τ_c Limit Using the Second Representation. In the regime of short τ_c, the FPE, equation 4.13, is employed to find the output firing rate. Although the set of equations 2.1, 4.11, and 4.12 generates only positive exponential correlations, we use them because its associated FPE can be solved perturbatively in powers of $k = \sqrt{\tau_c/\tau_m}$ and $\sqrt{\alpha}$. We have found the FPE, equation 4.7, including both positive and negative correlations too involved to be studied in the small k limit. Although the firing rate computed in this limit from the FPE 4.13 is derived only for positive correlations, when the same formula is employed for negative correlations, one finds an excellent agreement with the numerical results. This fact suggests that the analytical continuation of our formula to negative correlations ($\alpha < 0$) could match the true expression for that case.

---

[5]Note that the function within the brackets can be expressed in terms of the error function, similar to equation 5.4.

Even when using the FPE, equation 4.13, valid for positive correlations, the short τ_c expansion is not easy to obtain. This is because of the self-consistency condition, equation 4.20, which is hard to deal with. However, if the correlation time τ_c is short compared to the refractory time τ_{ref} ($\tau_{ref} \gg \tau_c$), the escape probability density flux can be written as (Doering, Hagan, & Levermore, 1987)

$$J_\alpha(y) = \nu_{out}\, \frac{e^{-y^2/2}}{\sqrt{2\pi}}, \tag{5.12}$$

which solves automatically conditions 4.19 and 4.20. This approximation is good because after a spike, the variable y approaches its gaussian stationary distribution in a time τ_c, which we are taking shorter than τ_{ref}.

We now look for a solution of the FPE 4.13 of the form

$$P_\alpha(x, y) = f_0(x, y) + k f_1(x, y) + O(k^2), \tag{5.13}$$

and at the same time we expand the escape probability density flux J_α in powers of k or, equivalently, the unknown output firing rate as

$$\nu_{out} = \nu_{eff} + k\nu_1 + O(k^2). \tag{5.14}$$

It can be shown that the solution $f_1(x, y)$ obtained from the perturbative expansion does not satisfy the vanishing boundary condition 4.18 (see appendix E). To address this problem, we extend the formalism described in Doering et al. (1987) to solve the short τ_c limit. As in Doering et al. (1987), our problem does not have a perturbative solution for short τ_c, and it is necessary to solve a boundary layer problem. Details of these calculations are given in appendix E. Briefly, the solution $P_\alpha^{total}(x, y)$ is obtained as the sum of the perturbative and an additional solution, valid close to the threshold, that we call boundary solution $f_1^b(x, y)$:

$$P_\alpha^{total}(x, y) = f_0(x, y) + k[f_1(x, y) + f_1^b(x, y)] + O(k^2). \tag{5.15}$$

It is now possible to satisfy condition 4.18 up to order k. Finally, the firing rate up to order k can be calculated using condition 4.17, resulting in

$$\nu_{out} = \nu_{eff}(\alpha) - \alpha\sqrt{\tau_c \tau_m}\,\nu_0^2\, R(\hat{\Theta}) \,, \tag{5.16}$$

where ν_0 is defined as in equation 5.4 and

$$\nu_{eff}^{-1}(\alpha) = \tau_{ref} + \sqrt{\pi}\,\tau_m \int_{\hat{H}_{eff}}^{\hat{\Theta}_{eff}} dt\, e^{t^2}(1 + \mathrm{erf}(t)). \tag{5.17}$$

Table 1: Analytical Expressions for the Output Firing Rate of an LIF Neuron Receiving Exponentially Correlated Inputs with Magnitude α and Correlation Timescale τ_c for the Two Representations of the Current in Both the Short and Long τ_c Limits.

	First Representation	Second Representation
Short τ_c	Not found	$\nu_{out} = \nu_{eff}(\alpha) - \alpha\sqrt{\tau_c\tau_m}\nu_0^2 R(\hat{\Theta})$, equation 5.16 Valid for small and positive α, and exact for all positive α when $\tau_c = 0$
Long τ_c	$\nu_{out} = \nu_0 + \frac{\alpha}{\tau_c}C$, equation 5.5 Valid for small α, positive and negative	$\nu_{out} = \frac{1}{\sqrt{2\pi}\tau_m}\int_{-\infty}^{\infty} dy\, e^{-\frac{y^2}{2}}$ $\left[\int_{\sqrt{2}\hat{H}-\gamma y}^{\sqrt{2}\hat{\Theta}-\gamma y} du\, e^{\frac{u^2}{2}} \int_{-\infty}^{u} dv\, e^{-\frac{v^2}{2}}\right]^{-1}$, with $\gamma = \sqrt{\alpha\tau_m/\tau_c}$, equation 5.11 Valid for all (even large) positive α

The effective reset and threshold potentials are defined as $\hat{\Theta}_{eff} = \frac{\Theta - \mu\tau_m}{\sigma_{eff}\sqrt{\tau_m}}$ and $\hat{H}_{eff} = \frac{H - \mu\tau_m}{\sigma_{eff}\sqrt{\tau_m}}$. An important implication of equation 5.16 is that when $\tau_c = 0$, the output rate is $\nu_{eff}(\alpha)$, equivalent to that of an LIF neuron receiving an uncorrelated input (white noise) with an effective signal variance,

$$\sigma_{eff}^2 = \sigma_w^2(1 + \alpha). \tag{5.18}$$

In this case, the solution is exact for all α. When $\tau_c \neq 0$, it is correct only for small values of both k and $\alpha > 0$. This expression indicates that when the correlation time is zero, the effect of the input correlations is to increase the white noise variance by a factor equal to $1 + \alpha$.

A general expression for the firing rate of any IF neuron is presented in appendix F. Again, for $\tau_c = 0$, the firing rate is that of the IF neuron with input white noise but with a renormalized variance as in equation 5.18. From this maximum firing rate at optimal synchronization, the firing rate decreases as $-\sqrt{\tau_c}$ for fixed α (see equation F.4, analogous to equation 5.16 for a LIF neuron), showing that this large sensitivity to variations in the correlation time of the inputs is a general property of IF neurons.

6 Summary of the Analytical Results

The analytical results, obtained in the first and second representations of the current, and in the short and long τ_c limits, along with the conditions on which they are valid, are summarized in Table 1.

The second representation allows calculating the firing rate for both short and long τ_c, while the first representation allows the calculation of the firing rate only for long τ_c. In Moreno et al. (2002) we used the second representation to obtain the firing rate for short τ_c, and therefore the expression shown

here is the same at that found there. On the other hand, using the second representation for long τ_c, here we have been able to find a new expression for the firing rate, equation 5.11, which can be applied for arbitrarily large α, while that found in Moreno et al. (2002) using the first representation, equation 5.5, could be applied only for small α. The expressions valid for long τ_c, equations 5.5 and 5.11, are in fact equivalent when the limit $\alpha \to 0$ is taken (see appendix D). Note, however, that equation 5.5 can be employed for negative α, while equation 5.11 can be used only for positive α.

7 The Effect of Correlations on the Firing Response of Spiking Neurons

In this section we take advantage of the machinery developed in the previous sections. First, the prediction of the firing rate as a function of the timescale and magnitude of input correlations is used to study the role of synchrony on the stationary firing response of an LIF neuron. Second, we study the firing response to modifications of the correlation magnitude. Numerical solutions of the voltage and noise equations to generate exponentially correlated noise are employed in this case.

7.1 Stationary Firing Response. Although we have calculated the output firing rate in both the limit $\tau_c \ll \tau_m$ and $\tau_c \gg \tau_m$, before the effect of τ_c and α on the firing rate is described, we develop an interpolation procedure that allows us to use a single expression for all values of τ_c. The interpolating curves have been determined by setting the firing rate in the short correlation time range ($\tau_c < \tau_m$) as

$$\nu_{out} = \nu_{eff} + A_1 \sqrt{\tau_c} + A_2 \, \tau_c, \tag{7.1}$$

where A_1 and A_2 are unknown functions of α and of the neuron and input parameters, while in the long correlation time limit ($\tau_c > \tau_m$), the expression given in equation 5.5,

$$\nu_{out} = \nu_0 + \alpha C / \tau_c, \tag{7.2}$$

was used. The functions A_1 and A_2 are determined by interpolating these two expressions with conditions of continuity and differentiability at a convenient interpolation point $\tau_{c,inter} \sim \tau_m$. Although we have calculated analytically the function A_1 (see equation 5.16) for small α, this procedure takes into account higher-order corrections that match more accurately the observed data for larger values of α as those used in some of our simulations (see below). Therefore, equations 7.1 and 7.2 provide an analytical formula for the output firing rate of an LIF neuron receiving exponentially correlated input valid for all τ_c.

We have performed numerical simulations of an LIF neuron driven by gaussian exponentially correlated input using equations 2.1, 4.1, and 4.2. We use them to check the analytical results given in equations 5.5, 5.11, and 5.16 and validate the interpolation made between the regimes of short and long τ_c, provided by equations 7.1 and 7.2. When positive correlations are considered ($\alpha > 0$), the interpolation procedure is robust against changes in μ and σ_w^2. Crucially, the interpolating point $\tau_{c,inter} \sim \tau_m$ does not vary too much, so that it can be maintained approximately fixed for all input parameters. For negative correlations, we have found it more convenient to add to the expansion in equation 7.2 an extra term: $\nu_{out} = \nu_0 + \alpha \, C/\tau_c + B_1/\tau_c^2$. This expression is then made to match at $\tau_{c,inter} \sim \tau_m$, the short τ_c regime given by the equation $\nu_{out} = \nu_{eff} + B_2\sqrt{\tau_c}$.

This interpolation is compared with simulation results in Figure 6, providing good fit. The firing rate increases as τ_c decreases (at fixed positive α). This corresponds to the intuitive result that positive correlations between the presynaptic events produce a larger enhancement in the output firing rate as the temporal window over which they occur decreases. On the other hand, when negative correlations are present in the input, the effect of τ_c is reversed: the firing rate increases as τ_c increases. Negative correlations produce a deficit in current fluctuations that reduces the firing rate. This deficit is not noticeable if τ_c is very long compared with τ_m. These results show that correlations with fixed magnitude α have different effects on a target neuron depending on the value of their correlation timescale. Correlations are not perceived by neurons if the temporal precision they occur at is larger than the membrane time constant of those neurons. As it can be appreciated in Figure 6, when τ_c is of the order of 40 ms (twice longer than τ_m), the output firing rate of the neuron approaches the firing rate obtained by an input without correlations ($\alpha = 0$, dashed-dotted line). Only if $\tau_c < \tau_m = 20$ ms is the presence of correlations noticeable. As noted above, this implies that from the point of view of the output firing rate, correlations in the input can be neglected (a white noise input description is appropriate) when τ_c is significantly longer than τ_m (note, however, that there is not an absolute value of τ_c for which correlations can be neglected; rather, this value will increase with α).

In Figure 7 we use the predictions of equations 5.5 and 5.11 valid for long τ_c. Here, large values of correlation magnitude, α, are used. The predictions are compared with simulations of neurons in the subthreshold (left) and the suprathreshold (right) regimes. The subthreshold and suprathreshold regimes are defined by $\mu\tau_m < \Theta$ and $\mu\tau_m > \Theta$, respectively, and they correspond to the fluctuation and drift-dominated regimes. The prediction by equation 5.11 is very good even for intermediate $\tau_c \sim \tau_m$ in both regimes. In contrast, the firing rate for long τ_c given in equation 5.5 provides poorer fits (dotted line in the left panel) in the subthreshold regime and even poorer in the suprathreshold regime when very large values of α are used
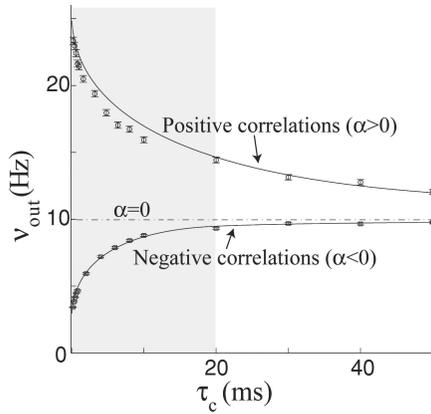
Figure 6: Theoretical predictions (lines) and simulation results (points) for the output firing rate of an LIF neuron driven by exponentially correlated inputs as a function of the correlation timescale. Here we use equation 7.1 for short τ_c and equation 7.2 for long τ_c, along with a continuous and smooth interpolation between the two limits (the interpolation is made at an intermediate $\tau_{c,inter} \sim \tau_m$). The rate decreases when the input correlations are positive ($\alpha > 0$, upper curve) and increases when correlations are negative ($\alpha < 0$, lower curve). When there are no correlations ($\alpha = 0$), the neuron fires at a rate of 10 Hz (dashed-dotted line). Maximum rate differences relative to the rate with no input correlations are attained when $\tau_c = 0$, that is, when the input correlation is exquisitely precise. Differences are substantial whenever the correlation time is shorter than the membrane time constant of the neuron ($\tau_m = 20$ ms for this case; shaded region). When the correlation time becomes longer than τ_m, relative changes are much smaller, and the neuron becomes less sensitive to the input correlations. Correlation magnitudes are $\alpha = 8$ (upper curve) and $\alpha = -0.75$ (lower curve), and interpolations between the short and long τ_c theoretical predictions were performed at the interpolating time $\tau_{c,inter} = 40$ ms and 20 ms, respectively. Other parameters are $\tau_{ref} = 0$ ms, $\Theta = 1$ (in arbitrary units), $H = 0$, $\mu = 42\,\mathrm{s}^{-1}$, $\sigma_w^2 = 2\,\mathrm{s}^{-1}$. Although the short τ_c expansion requires $\tau_{ref} \neq 0$, the simulation shows that this prediction is good even for zero τ_{ref}.

(not shown). This is because the second prediction of the firing rate was obtained for fixed α.

The figure also shows that the effect of correlations is quite different for a neuron receiving subthreshold or suprathreshold inputs. For subthreshold inputs, positive correlations always increase the firing rate relative to the case without correlations, and the firing rate decreases as the timescale of correlations becomes broader. However, for suprathreshold inputs, a different qualitative behavior is observed, at least for small white noise variances. Positive correlations with long enough τ_c give an output firing
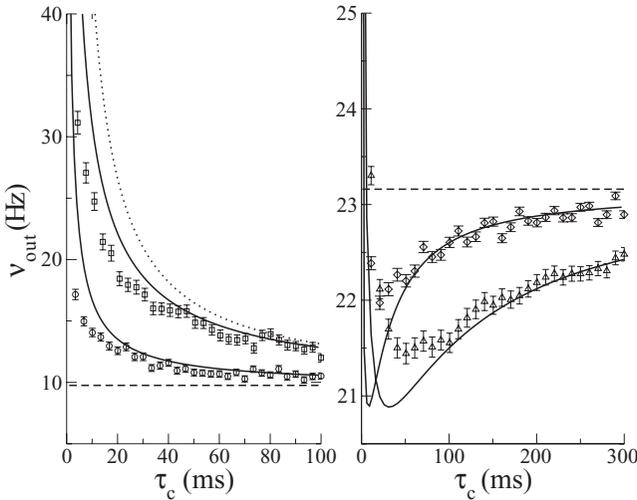
Figure 7: Theoretical predictions and simulation results for the firing rate of an LIF neuron as function of the correlation timescale for the sub- (left) and the suprathreshold regimes (right). Here we use equations 5.5 and 5.11, valid for long τ_c. For the subthreshold regime, the effect of increasing the correlation time is always to decrease the rate. However, for the suprathreshold regime and when the input noise is small, the effect is the opposite for long τ_c. As the input noise increases, this effect disappears, and the curve becomes as in the subthreshold regime (data not shown). The theoretical predictions (full lines) are obtained using the firing rate given in equation 5.11 without any interpolation, and the discrete points are the simulation results with the same parameters as in the theoretical curves. Parameters for the subthreshold regime are $\mu = 0$ Hz, $\sigma_w^2 = 50.5$ Hz, and $\alpha = 4$ (top full line and squares), $\alpha = 1$ (bottom full line and circles), and $\alpha = 0$ (straight line). The dotted line has the same parameters as the top full line, but it has been obtained from the expression of the rate in equation 5.5. Notice that the prediction from equation 5.11, strictly valid only for long τ_c, is also good even when $\tau_c \sim \tau_m$, and it is better than that provided by equation 5.5 for all τ_c. Parameters for the suprathreshold regime are $\mu = 100.7$ Hz, $\sigma_w^2 = 0.05$ Hz, and a very large correlation strength $\alpha = 36$ (bottom line and triangles), a moderate correlation strength $\alpha = 9$ (intermediate line and diamonds), and $\alpha = 0$ (straight line). The other parameters are as in Figure 6, except for $\tau_m = 10$ ms.

rate smaller than the basal rate without correlations, although this effect is very small (notice the large values of α that have been used). A minimum firing rate is attained when the correlation timescale is longer than the membrane time constant of the neuron, and the exact value of τ_c at which the minimum occurs is roughly predicted by the analytical formula, 5.11. When the white noise variances become larger, this counterintuitive

effect of correlations disappears, and the profile is much more similar to the subthreshold case, but with much smaller correlation-induced changes.

Overall, this analysis shows that neurons are more sensitive to correlations in the subthreshold than in the suprathreshold regime, which is not surprising, since in the first regime, spiking is driven by input fluctuations and correlations enhance them (Moreno et al., 2002; Salinas & Sejnowski, 2001).

7.2 Transient Firing Response. Another important question is how fast a neuron can respond to *pure* changes in the correlation magnitude α, that is, when both the afferent mean current and white noise variance σ_w^2 are fixed. In our work (Moreno et al., 2002), we have shown that changes in correlation magnitude can be transmitted very fast by the firing rate of spiking neurons even when the timescale of those correlations is quite large. Those firing responses are also compared here with the response to sudden jumps in mean input current.

Let us write the instantaneous firing rate for the time-dependent FPE, in either the first or second representation, as (see equation 4.20)

$$v_{out}(t) = -\frac{\sigma_w^2(t)}{2} \frac{\partial}{\partial V} \int_{-\infty}^{\infty} dw\, P(V, w, t)|_{V=\Theta}. \tag{7.3}$$

For clarity, we have come back to the physical quantity V and use its distribution $P(V, w, t)$ ($w = z, y$). A similar equation for the instantaneous firing rate of a one-dimensional FPE has been used by Silberberg, Bethge, Markram, Pawelzik, & Tsodyks (2004) to predict that any instantaneous modification in the white noise variance, $\sigma_w^2(t)$, produces an immediate change in the output firing rate of the neuron. Besides, as we have shown before, the exact form of equation 7.3 for $\tau_c = 0$ corresponds to a neuron receiving (uncorrelated) input white noise with effective variance $\sigma_{eff}^2 = \sigma_w^2(1 + \alpha)$, equation 3.16. This gives (Moreno et al., 2002)

$$v_{out}(t) = -\frac{\sigma_{eff}^2(t)}{2} \frac{\partial}{\partial V} \int dw\, P(V, w, t)|_{V=\Theta}. \tag{7.4}$$

Now it is clear that any change in α will produce an immediate change in $v_{out}(t)$, because the distribution $P(V, t) = \int dw\, P(V, w, t)$ can experience only a smooth change (notice that the trajectories generated by the equations for V—e.g, see equations 2.1, 4.1, and 4.2—are continuous under changes in α). This means that when $\tau_c = 0$, changes in the correlation magnitude (α) will be felt immediately by the firing response of the neuron. By analyticity arguments, the response under changes in α will be also fast for nonzero τ_c.
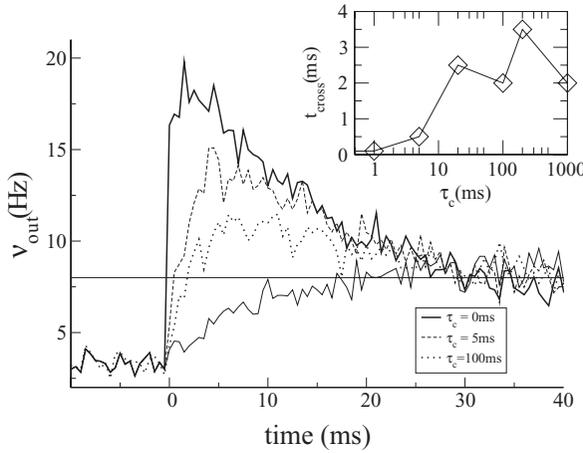
Figure 8: Averaged transient firing responses of an LIF neuron to changes in the input statistics. Below $t = 0$ the input is white noise ($\alpha = 0$) with $\mu = 16\,\mathrm{s}^{-1}$ and $\sigma_w^2 = 0.81\,\mathrm{s}^{-1}$. Upper curve: instantaneous response when σ_w^2 is increased up to $\sigma_w^2 = 3.8\,\mathrm{s}^{-1}$. Second (third) curve: quick response to correlation changes, with $\tau_c = 5$ ms (100 ms) and $\alpha = 6.8$ (52.3). Bottom curve: slow response when μ is changed from $\mu = 16.9\,\mathrm{s}^{-1}$ to $\mu = 19.9\,\mathrm{s}^{-1}$ and σ_w^2 is kept constant. These values were chosen so that the evoked firing rates in the final steady state are roughly the same (~ 8 Hz, straight line). Inset: Time when the firing rate response for the first time reaches the value of the final stationary rate as a function of τ_c. When the correlation timescale is very short, t_{cross} is very small, and it saturates for long τ_c. Neuron parameters are $\tau_m = 50$ ms, $\tau_{ref} = 0$, $\Theta = 1$, and $H = 0$ (dimensionless).

These predictions have been tested with numerical simulations, whose results are shown in Figure 8. Initially the input statistics is white noise, and some time later, either the mean current μ (bottom curve), or the white noise variance σ_w (upper curve), or the correlation amplitude α (two intermediate curves) is changed independently. Changing the mean current abruptly produces only a slow response with a timescale on the order of the membrane time constant. However, in the absence of correlations, the firing rate changes instantaneously under a sudden modification in the variance of the injected current (σ_w^2). In agreement with our prediction, for short τ_c, the response is also very quick when the correlation changes from $\alpha = 0$ to a positive value. To quantify how fast the response is, we computed the time t_{cross} at which the instantaneous rate reaches for the first time the value of the final stationary firing rate. The inset in Figure 8 shows that as a function of τ_c, t_{cross} initially grows, but it soon saturates at about 3 ms, even when τ_c is several hundred milliseconds long. Thus, the correlation time is not a limiting factor for fast transmission of information contained

in correlation changes. This result shows that information carried by correlated input patterns can be transmitted with a timescale that is not limited by the membrane time constant, which is not the case for signals embedded in the mean input current (Moreno et al., 2002). Rudolph and Destexhe (2001) show that correlation changes can be followed very rapidly by a spiking neuron. Because they consider the case of perfect synchrony, $\tau_c = 0$, their conclusions are similar to those of Silberberg et al. (2004), because the case $\tau_c = 0$ corresponds to a simple renormalization of the current variance (σ_w^2), as we have explained before (see equation 3.16).

These results show that fast information transmission in cortex using spike correlations is theoretically possible. As we have shown, changing the mean afferent current produces slow responses if the neuron is in the subthreshold regime, because the mean current has to be integrated in a timescale τ_m. However, because of their fast transmission rate, correlation modulations can be an ideal candidate for transmitting information rapidly. The fact that changes in μ do not evoke rapid responses does not mean that rate codes are inefficient for transmitting information rapidly. Rather, changes in the firing rate of "noisy" input spike trains (as in a Poisson train) involve changes in both μ and fluctuations σ_w (Ricciardi, 1977) and indeed also in α (see their definitions in equations 3.15). Such white noise variance and correlation magnitude modulations can be transmitted very fast, while the mean current modulations produce a slower response. Therefore, an increase in the firing rate of an irregularly spiking presynaptic population will produce an output rate change that contains information in at least two different timescales (one fast and another slow).

8 Discussion

In this article, we have provided and thoroughly analyzed a theoretical framework to understand how temporal correlations affect the output firing response of neurons. The main qualitative results we found are:

- The neuron's output rate is very sensitive to precisely synchronized inputs with $\tau_c < \tau_m$.
- The response decreases (increases) with the timescale τ_c for positive (negative) correlations and increases (decreases) with their magnitude α.
- The neuron response to sudden changes in the size of the correlations is very fast regardless of the magnitude of the change and on the correlation time.

An important question is how our results can be incorporated into the modeling of neural networks. Temporal and spatial correlations are presumably relevant to correctly describe the dynamics of realistic recurrent neuronal networks. Recently, we (Renart et al., 2007) proposed an extended mean field approach to determine the firing rate and spiking variability of

a large network of LIF neurons. In classical mean field theory, the neurons in the network are assumed to fire in a Poisson and independent manner (Amit & Brunel, 1997b; Renart, Brunel, & Wang, 2003), so that the only free dynamical parameter in the dynamics of an homogeneous population of neurons is its population firing rate. Our extension goes beyond the classical mean field theory by adding as a free parameter the spiking variability of the network, that is, the coefficient of variation of the interspike intervals, CV. Then the firing rate as well as the variability of the network can be studied without the assumption that the spike trains are Poisson, corresponding to the case $CV = 1$. In particular, stationary states with $CV > 1$ would correspond to states of high spiking variability, while stationary states of the network with $CV < 1$ would correspond to more regular spiking regimes of the neuronal dynamics. The formalism presented in Renart et al. (2007) is based on the result that when the correlation time of the spike trains is short enough ($\tau_c \ll \tau_m$), then the input variability can be expressed as (see equations 5.18 and 3.15; Moreno et al., 2002)

$$\sigma_{eff}^2 = J_E^2 \, N_E \, CV_E^2 \, \nu_E + J_I^2 \, N_I \, CV_I^2 \, \nu_I, \tag{8.1}$$

assuming that there are no cross-correlations ($\rho = 0$). Since the output firing rate and the output CV of an integrate-and-fire neuron can be calculated exactly when the input is white noise (Ricciardi, 1977), then a mapping between the input rates and CV, and the output rates and CV, can be constructed as

$$\nu_{out} = f_\nu(\nu_{in}, CV_{in})$$
$$CV_{out} = f_{CV}(\nu_{in}, CV_{in}), \tag{8.2}$$

where the functions f_ν and f_{CV} are the expressions for the output firing rate and CV of the IF neuron receiving white noise input. These equations define an input-output mapping of the neuronal dynamics with independent variables ν and CV. Therefore, under the conditions described above, a mean field theory for the dynamics of the mean and variability of the spiking response can be formulated. Doiron et al. (2006) have also recently used our renormalization technique of the input variance, as defined in equations 8.1 and 8.2, to describe the transmission of the activity of nonleaky IF neuron in feedforward networks. As we have said above, Renart et al. (2007) have addressed the problem of self-consistency in firing rate and CV in recurrent networks of LIF neurons. Other work has also studied this problem using different approaches to find self-consistent equations for the spiking variability of the network (Lerchner et al., 2006).

However, further extensions of our mean field theory (Renart, Moreno, de la Rocha, Rolls, & Parga, 2001; Moreno et al., 2002; Renart et al., 2007) are required to consider in a self-consistent way the second-order statistics

of the neuronal activity in spiking recurrent networks. A first step has been made in Moreno-Bote and Parga (2006), where the auto- and cross-correlation functions of the output response of a pair of spiking neurons receiving independent as well as common sources of noise have been analytically determined.[6] The self-consistent treatment of spike cross-correlation functions (i.e., the input and output cross-correlation functions should also match each other) to describe more realistic recurrent neuronal networks seems to be an unavoidable step to understand how neurons' interactions give rise to network behaviors. The problem can be formally stated as follows: find the set of mean field equations mapping the input values of the relevant dynamical variables of the network (firing rate, F_N and ρ) to their output values:

$$\nu_{out} = f_\nu(\nu_{in}, F_{N,in}, \rho_{in})$$

$$F_{N,out} = f_{F_N}(\nu_{in}, F_{N,in}, \rho_{in})$$

$$\rho_{out} = f_\rho(\nu_{in}, F_{N,in}, \rho_{in}).$$

This set of equations is now available at least for an LIF neuron receiving colored noise (Moreno-Bote & Parga, 2006).

In this work, we have considered decaying (exponential) correlations, while in cortex, damped oscillatory cross-correlograms are also observed (see, e.g., Vaadia et al., 1995; Riehle et al., 1997; Fries et al., 1997). This problem could be addressed by introducing a stochastic current that obeys a second-order equation driven by white noise: the well-known damped oscillator. A current generated in this way can have a cross-correlogram with exponentially decaying oscillations, with frequency and damping value controlled by the parameters of the equation. Although this problem is relevant, we do not study it here, since the new system would involve solving a more complicated FPE, now with three independent variables.

Here we have not studied neuron models with conductance-based synapses either. However, an analogous expression for the firing rate at long τ_c can be obtained if the noise enters multiplicatively instead of additively. (Although we do not present the derivation here, the FPE for neuron models with conductance-based synapses can be solved using the techniques in appendix D.) Qualitatively, the effect of the correlation magnitude and correlation timescale in conductance-based models is not different from their effects in current-based models. Note, however, that in the first case, correlations are strongly effective only when τ_c is shorter than the effective membrane time constant of the neuron, which now depends on the total conductance (see, e.g., Moreno-Bote & Parga, 2005).

---

[6]For different approximations of this computation see Lindner, Doiron, and Longtin (2005) and Masuda (2006).

We have modeled input spike trains as delta functions (point processes) without any further temporal synaptic filtering. This means that the cross-correlation function of the total input current displays a delta function at zero time lag, as shown in equation 3.14. When the input spike trains are filtered by synapses with a finite synaptic time constant τ_s, they generate a train of exponential-like current waveforms into the neuron. The delta function in the correlation function, equation 3.14, then becomes an exponential with the same time constant as that of the synaptic filter, τ_s (see, e.g., Brunel & Sergi, 1998; Moreno-Bote & Parga, 2004). At the same time, the exponential term in the correlation function results after filtering in two additional exponentials, with time constants τ_c and τ_s, respectively. Then the result of (linearly) filtering correlated input spike trains is an input current whose correlation function has two kinds of exponentials, each with a different time constant (τ_c and τ_s). Particular cases of this interesting problem (e.g., when the two timescales are disparate) could be addressed analytically by using the techniques developed to study simultaneous fast and slow synaptic filtering (Moreno-Bote & Parga, 2004).

Two differences are expected when synaptic filters are present in the model. First, synapses filter out fluctuations in the input whose timescale is shorter than τ_s and convert them into fluctuations with timescale τ_s. Fluctuations that are slower than τ_s will pass the synapses. Therefore, fast fluctuations produced by precise input synchronization (i.e., short $\tau_c \leq \tau_m$) will not be seen by the neuron: effectively, the sharp synchronization of timescale τ_c is converted into a coarser synchronization with timescale τ_s. Then we expect that for $\tau_c < \tau_s$, the firing rate will depend very little on τ_c in that range. However, when $\tau_c > \tau_s$, the rate versus τ_c curve will decay fast until τ_c crosses τ_m, after which the effect of input correlation on the rate will be small, similar to Figure 6. Second, filters introduce a delay in the transient firing response to sudden increases of input synchrony. We have run simulations with fast filters ($\tau_s \leq 5$ ms) and found that the response was still fast and was delayed by the time constant of the synapses.

In future work, it would be desirable to develop a complete theory that describes the firing statistics of integrate-and-fire neurons with conductance-based synapses and finite synaptic timescales driven by correlated spike trains. The effect of input correlations in this more complex system could be evaluated by extending and combining the techniques developed in this and in Moreno et al. (2002), Moreno-Bote & Parga (2004, 2005, 2006), and Renart et al. (2007).

Appendix A: Numerical Procedures

The equations for the voltage of the integrate-and-fire neuron and the correlated gaussian noise are numerically solved using a simple Euler integration procedure, along with a Monte Carlo method. This procedure gives an excellent estimate of the output firing rate (time dependent or independent),

which can be compared to the theoretical predictions. As an example, the dynamics of the voltage of a LIF neuron in equation 2.1 with the current $I(t)$ defined in equations 4.1 and 4.2 is integrated using a small time step ($\delta t = 5\ 10^{-4} ms \ll \tau_m$) as

$$V(t + \delta t) = V(t) - \frac{V(t)}{\tau_m}\delta t + I(t)\delta t, \tag{A.1}$$

$$I(t) = \mu + \sigma_w \frac{\omega(t)}{\sqrt{\delta t}} + \sigma_w \frac{\beta}{\sqrt{2\tau_c}} z(t), \tag{A.2}$$

$$z(t + \delta t) = z(t) - \frac{z}{\tau_c}\delta t + \sqrt{\frac{2}{\tau_c}}\omega(t)\sqrt{\delta t}, \tag{A.3}$$

with the reset condition $V = H$ after a spike is generated (when $V \geq \Theta$). The initial value of the noise variable z is that at the time of the previous spike, z is not reset after each spike. The variable $\omega(t)$ is a random variable taking values $+1$ and -1 with equal probability $1/2$ at each time step δt, and being drawn independently from time step to time step. Therefore, $\langle \omega(t) \rangle = 0$, $\langle \omega^2(t) \rangle = 1$ and $\langle \omega(t)\omega(t') \rangle = 0$, where $t \neq t'$. This means that the quantity $\omega(t)/\sqrt{\delta t}$, which appears in the expression for the current $I(t)$ above, is an approximation to the delta function, since $\langle \omega(t)/\sqrt{\delta t} \rangle = 0$, $\langle \omega^2(t)/\delta t \rangle = 1/\delta t$, and $\langle \omega(t)\omega(t')/\delta t \rangle = 0$. The procedure described above is robust and converges to the true stationary process as δt decreases. The Monte Carlo simulations were run using Fortran90 custom code. Special care has to be taken in choosing an appropriate random generator for $\omega(t)$.

Appendix B: Derivation of the FPEs

FPE 4.7 is here derived for the set of equations

$$\dot{x}(t) = -\frac{x(t)}{\tau_m} + \sqrt{\frac{2}{\tau_m}}\eta(t) + \frac{\beta}{\sqrt{\tau_m \tau_c}} z(t)$$

$$\dot{z}(t) = -\frac{z}{\tau_c} + \sqrt{\frac{2}{\tau_c}}\eta(t), \tag{B.1}$$

corresponding to the first representation of the current. FPE 4.13 associated with the second representation of the current can be obtained using the same rules described in this section. More formal derivations of similar FPEs can be found in Ricciardi (1977) and Risken (1989).

The system defined by equations B.1 is fully described by the probability density function $P_\beta(x, z, t)$. This function expresses the probability density of having the neuron in the state (x, z) at time t. The FPE is an equation that

precisely describes the dynamics (i.e., time evolution) of such a density. A first step toward the derivation of the FPE consists in discretizing the time in the dynamics, as in appendix A. This leads to

$$x(t + \delta t) = x(t) - \frac{x(t)}{\tau_m}\delta t + \sqrt{\frac{2}{\tau_m}}\omega(t)\sqrt{\delta t} + \frac{\beta}{\sqrt{\tau_m \tau_c}}z(t)\delta t$$

$$z(t + \delta t) = z(t) - \frac{z}{\tau_c}\delta t + \sqrt{\frac{2}{\tau_c}}\omega(t)\sqrt{\delta t}, \qquad (B.2)$$

where δt represents an infinitesimal time increment, and $\omega(t)$ is a random variable taking values $+1$ and -1 with probability $p(w = \pm 1) = 1/2$ and drawn independently at every infinitesimal time step. The terms in equations B.2 proportional to $\sqrt{\delta t}$ are approximations of the delta functions in equations B.1 integrated during the infinitesimal time increment.

To determine the FPE associated with equations B.1, one has to relate the density at time $t + \delta t$, $P_\beta(x, z, t + \delta t)$, with the density at a previous time t, $P_\beta(x', z', t)$. First, we realize that the probability that we find a neuron in an infinitesimal square $\delta x'\delta z'$ around state (x', z') at time t has probability $P_\beta(x', z', t)\delta x'\delta z'$. Second, the state square centered at (x', z') with surface $\delta x'\delta z'$ will be projected at the successive time $t + \delta t$ into another square centered at (x, z) with surface $\delta x\delta z$ close to the previous one, obeying the rules defined in equations B.2. Therefore, by conservation of the probability, we have that

$$P_\beta(x, z, t + \delta t)\, \delta x\delta z = \sum_{w=\pm 1} p(w)\, P_\beta(x'(w), z'(w), t)\, \delta x'\delta z', \qquad (B.3)$$

where

$$x'(w) = x + \frac{x}{\tau_m}\delta t - \sqrt{\frac{2}{\tau_m}}\omega\sqrt{\delta t} - \frac{\beta}{\sqrt{\tau_m \tau_c}}z\delta t$$

$$z'(w) = z + \frac{z}{\tau_c}\delta t - \sqrt{\frac{2}{\tau_c}}\omega\sqrt{\delta t}.$$

Notice that the states $(x'(w), z'(w))$ $(w = \pm 1)$ defined above are the only ones from where one can arrive at the state (x, z) after an infinitesimal amount of time δt. In addition, the box around state (x', z') is compressed to the box around the final state (x, z) by a factor $\delta x\delta y = (1 - \delta t/\tau_m)(1 - \delta t/\tau_c)\delta x'\delta y'$, given by the decaying term in equations B.1.

After expanding the densities in equation B.3 in powers of $\sqrt{\delta t}$, we find that all terms that are order $\sqrt{\delta t}$ are equal to zero (since $\langle \omega \rangle = 0$), while

the terms order δt do not vanish (either they do not depend on ω, or they are proportional to ω^2, and therefore $\langle \omega^2 \rangle = 1$). After equaling the terms at $O(\delta t)$, one obtains the FPE

$$\tau_m \frac{\partial}{\partial t} P_\beta(x, z, t) = \left[L_x + \frac{L_z}{k^2} + \frac{2}{k} \frac{\partial}{\partial x} \left(\frac{\partial}{\partial z} - \frac{\beta z}{2} \right) \right] P_\beta(x, z, t). \qquad (B.4)$$

In the time-independent case, $\frac{\partial}{\partial t} P_\beta(x, z, t) = 0$. However, to establish a stationary probability density function that does not depend on time, the probability density flux escaping at threshold (probability density flux in the direction of the variable x calculated at threshold) should be reinjected into the reset voltage. This enforces conservation of the total probability, that is, $\int \int dx dz \rho(x, z, t) = 1$ at all times, and leads to the self-consistent stationary FPE 4.7.

Appendix C: Long τ_c Expansion Using the First Representation

Here we detail the main steps for calculating the firing rate in equation 5.5. Introducing the expansions 5.1 and 5.2 in equation 4.7, we obtain

$$L_x h_n + L_z h_{n-2} + 2 \frac{\partial}{\partial x} \left(\frac{\partial}{\partial z} - \frac{\beta z}{2} \right) h_{n-1} + \tau_m \delta(x - \sqrt{2}\hat{H}) J_{\beta, n-1}(z) = 0$$

$$\qquad (C.1)$$

($h_n \equiv 0$ for $n < 0$). The solution to these equations is obtained order by order in such a manner that conditions 4.17 and 4.20 are satisfied. After solving them up to order k^2 using conditions 4.18 and 4.20 and the fact that the h_n's have to be normalizable, we obtain that

$$h_0(x, z) = k_0(x) J_{\beta, 0}(z),$$

$$h_1(x, z) = k_0(x) J_{\beta, 1}(z) + k_1(x) \left(2 \frac{\partial}{\partial z} - \beta z \right) J_{\beta, 0}(z),$$

$$h_2(x, z) = k_0(x) J_{\beta, 2}(z) + k_1(x) \left(2 \frac{\partial}{\partial z} - \beta z \right) J_{\beta, 1}(z)$$

$$+ k_2(x) \left(2 \frac{\partial}{\partial z} - \beta z \right)^2 J_{\beta, 0}(z), \qquad (C.2)$$

where the functions k_i are

$$k_0(x) = \tau_m e^{-\frac{x^2}{2}} \int_x^{\sqrt{2}\Theta} dy \, e^{\frac{y^2}{2}} H(y - \sqrt{2}\hat{H}),$$

$$k_1(x) = e^{-\frac{x^2}{2}} \int_x^{\sqrt{2}\hat{\Theta}} dy\, e^{\frac{y^2}{2}} k_0(y),$$

$$k_2(x) = e^{-\frac{x^2}{2}} \int_x^{\sqrt{2}\hat{\Theta}} dy\, e^{\frac{y^2}{2}} k_1(y).$$

The coefficients $J_{i,\beta}(z)$ in equation C.2 still have to be calculated. This is done by integrating first the h_n's over x from $-\infty$ to $\sqrt{2}\hat{\Theta}$ and using condition (4.21). After using condition 4.19, we find

$$J_0(z) = v_0 Z_0(z),$$

$$J_1(z) = \frac{(2+\beta)v_0 \int_{-\infty}^{\sqrt{2}\hat{\Theta}} dx\, k_1(x)}{\int_{-\infty}^{\sqrt{2}\hat{\Theta}} dx\, k_0(x)}\, z\, Z_0(z),$$

$$J_2(z) = \left[\frac{\alpha}{\tau_m} C + \frac{\alpha C}{\beta^2 \tau_m (1 - v_0 \tau_{ref})}(z^2 - 1) \right] Z_0(z),$$

$$C = \tau_m v_0^2 \left[\frac{\left(\int_{-\infty}^{\sqrt{2}\hat{\Theta}} dx\, k_1(x) \right)^2}{\int_{-\infty}^{\sqrt{2}\hat{\Theta}} dx\, k_0(x)} - \int_{-\infty}^{\sqrt{2}\hat{\Theta}} dx\, k_2(x) \right], \tag{C.3}$$

where $Z_0(z) = e^{-z^2/2}/\sqrt{2\pi}$. Finally, integrating again $J_{i,\beta}(z)$ over z gives the contributions to the output firing rate in equation 5.5. In the next section, we calculate the integrals appearing in parameter C in equation C.3.

C.1 Integrals. Here we present only some intermediate steps and the final results for the integrals appearing in C, equation C.3. The last two integrals can be expressed in terms of the function $R(t) = \sqrt{\frac{\pi}{2}} e^{t^2}(1 + \mathrm{erf}(t)) = e^{t^2} \int_{-\infty}^{\sqrt{2}t} ds\, e^{-s^2/2}$ as

1. $\displaystyle \int_{-\infty}^{\sqrt{2}\hat{\Theta}} dx\, k_0(x)$

    $$= \tau_m \int_{-\infty}^{\sqrt{2}\hat{\Theta}} dx\, e^{-\frac{x^2}{2}} \int_x^{\sqrt{2}\hat{\Theta}} dy\, e^{\frac{y^2}{2}} H(y - \sqrt{2}\hat{H}) = \frac{1 - v_0 \tau_m}{v_0}.$$

2. $\displaystyle \int_{-\infty}^{\sqrt{2}\hat{\Theta}} dx\, k_1(x) = \int_{-\infty}^{\sqrt{2}\hat{\Theta}} dx\, e^{-\frac{x^2}{2}} \int_x^{\sqrt{2}\hat{\Theta}} dy\, e^{\frac{y^2}{2}} k_0(x)$

    $$= \tau_m \int_{\sqrt{2}\hat{H}}^{\sqrt{2}\hat{\Theta}} dy\, e^{\frac{y^2}{2}} \int_{-\infty}^{y} dx\, e^{-\frac{x^2}{2}} (y - x) = \tau_m (R(\hat{\Theta}) - R(\hat{H})).$$

3. $$\int_{-\infty}^{\sqrt{2}\hat{\Theta}} dx k_2(x) = \int_{\sqrt{2}\hat{H}}^{\sqrt{2}\hat{\Theta}} \frac{\tau_m}{2} dy e^{\frac{y^2}{2}} \int_{-\infty}^{y} dx e^{-\frac{x^2}{2}} (y - x)^2$$

$$= \tau_m \left(\frac{\hat{\Theta}}{\sqrt{2}} R(\hat{\Theta}) - \frac{\hat{H}}{\sqrt{2}} R(\hat{H}) \right).$$

Appendix D: Long τ_c Expansion Using the Second Representation ——

In this section we derive the output firing rate formula 5.11 using the FPE
4.13. Here, we take the ratio $\gamma \equiv \sqrt{\alpha}/k$ to be a parameter independent of k,
that is, it is fixed. This will allow us to study the case of large α in the long
τ_c limit. From the FPEs 4.13 and 5.7, we develop a systematic expansion of
the probability distribution $P_\alpha(x, y)$ and the escape probability density flux
$J_\alpha(y)$ in powers of k^{-2} (see the expansion in equation 5.8), in which γ is
considered a fixed parameter independent of k. Inserting the expansion in
equation 5.8 into the FPE 5.7 produces

$$\left[L_x - \gamma y \frac{\partial}{\partial x} \right] r_n + L_y r_{n-1} + \tau_m \delta(x - \sqrt{2}\hat{H}) J_{\alpha,n}(y) = 0, \tag{D.1}$$

where $r_n \equiv 0$ if $n < 0$. For simplicity, the set of conditions 4.17 to 4.21 is used
here when $\tau_{ref} = 0$. Solving the zeroth order in equation D.1 with conditions
4.18 and 4.20 gives

$$r_{\alpha,0}(x, y) = \tau_m J_{\alpha,0}(y) e^{-\frac{(x-\gamma y)^2}{2}} \int_{x}^{\sqrt{2}\hat{\Theta}} du \, e^{\frac{(u-\gamma y)^2}{2}} H(u - \sqrt{2}\hat{H}), \tag{D.2}$$

where the escape probability density flux $J_{\alpha,0}(y)$ has yet to be determined.
This is done by using condition 4.21 with $\tau_{ref} = 0$ at zeroth order to obtain

$$J_{\alpha,0}(y) = \frac{1}{\sqrt{2\pi}\tau_m} e^{-\frac{y^2}{2}} \left[\int_{\sqrt{2}\hat{H}-\gamma y}^{\sqrt{2}\hat{\Theta}-\gamma y} du \, e^{\frac{u^2}{2}} \int_{-\infty}^{u} dv e^{-\frac{v^2}{2}} \right]^{-1}. \tag{D.3}$$

Repeating the same steps as above, the nth $(n > 0)$ order escape probability
density flux is found to be

$$J_{\alpha,n+1}(y) = \left[\int_{\sqrt{2}\hat{H}-\gamma y}^{\sqrt{2}\hat{\Theta}-\gamma y} du \, e^{\frac{u^2}{2}} \int_{-\infty}^{u} dv e^{-\frac{v^2}{2}} \right]^{-1}$$

$$\int_{-\infty}^{\sqrt{2}\hat{\Theta}} dx e^{\frac{-(x-\gamma y)^2}{2}} \int_{x}^{\sqrt{2}\hat{\Theta}} dv e^{\frac{(v-\gamma y)^2}{2}} L_y \int_{-\infty}^{u} dv r_n(v, y), \tag{D.4}$$

and the density r_n is computed as

$$r_n(x, z) = e^{\frac{-(x-\gamma y)^2}{2}} \int_x^{\sqrt{2}\hat{\Theta}} dv e^{\frac{(v-\gamma y)^2}{2}} L_y \int_{-\infty}^u dv r_{n-1}(v, y)$$

$$+ \tau_m J_{\alpha,n}(y) e^{-\frac{(x-\gamma y)^2}{2}} \int_x^{\sqrt{2}\hat{\Theta}} du\, e^{\frac{(u-\gamma y)^2}{2}} H(u - \sqrt{2}\hat{H}).$$

The zeroth-order rate is obtained by integrating over y the zeroth-order escape probability density flux in equation D.3. This gives the firing rate in equation 5.11. For fixed α, the parameter γ decreases as τ_c grows. In this limit, we could expand the zeroth-order firing rate in powers of γ. The firing rate obtained from this expansion has a dominant order k^{-2} ($O(\gamma^2)$). However, other contributions to the total firing rate at order k^{-2} could also come from the nonzeroth-order firing rate from the expansion 5.8. In particular, the first order ($n = 1$) rate in the expansion 5.8 is order k^{-2}. However, it is possible to see that an expansion in powers of γ in the term with $n = 1$ in equation D.4 also leads to an extra dominant order k^{-2}, and that multiplied by k^{-2} yields finally a correction to the firing rate bigger than $O(k^{-2})$. This finally proves that the leading correction to the firing rate for fixed α when τ_c approaches infinity is order k^{-2}, and it is given by the expansion of the zeroth-order rate 5.11. Naturally this expansion matches the output firing rate formula 5.5 for positive correlation magnitudes.

Appendix E: Short τ_c Expansion Using the Second Representation

E.1 The Free Solution. We introduce an expansion of the form 5.13 and 5.14 into FPE 4.13 and find the set of equations:

$$L_y f_0 = 0, \tag{E.1}$$

$$L_y f_1 = \sqrt{\alpha} y f_0, \tag{E.2}$$

$$L_y f_2 = -L_x f_0 + \sqrt{\alpha} y f_1 - \tau_m \delta(x - \sqrt{2}\hat{H}) v_{eff} Z_0(y), \tag{E.3}$$

$$L_y f_3 = -L_x f_1 + \sqrt{\alpha} y f_2 - \tau_m \delta(x - \sqrt{2}\hat{H}) v_1 Z_0(y), \tag{E.4}$$

where $Z_0(y) = e^{-y^2/2}/\sqrt{2\pi}$. After solving equation E.1, we find that the only normalizable solution is

$$f_0(x, y) = g_0(x) Z_0(y), \tag{E.5}$$

where g_0 has yet to be determined. The equation at order k gives the expression for f_1:

$$f_1(x, y) = \left[g_1(x) - \sqrt{\alpha} y \frac{\partial}{\partial x} g_0(x) \right] Z_0(y). \tag{E.6}$$

Again, g_1 is unknown. The equation at second order satisfies

$$L_y f_2(x, y) = -\alpha y g_1(x) Z_0(y)$$
$$- \left[L_x g_0(x) + \alpha \frac{\partial^2}{\partial x^2} g_0(x) - \tau_m \delta(x - \sqrt{2}\hat{H}) v_{eff} \right] Z_0(y). \tag{E.7}$$

Using that the integral $\int dy L_y f_2(x, y)$ has to equal zero in order for f_2 to be integrable, we can integrate equation E.7 over y and obtain the condition

$$\left[\frac{\partial}{\partial x} x + (1 + \alpha) \frac{\partial^2}{\partial^2 x} \right] g_0(x) + \tau_m v_{eff} \delta(x - \sqrt{2}\hat{H}) = 0. \tag{E.8}$$

This equation is the same as that obtained when solving the FPE for a LIF neuron driven by white noise input (Ricciardi, 1977), but where the variance of the noise has been renormalized by a factor $1 + \alpha$. This equation is solved exactly for all α using condition 4.18,

$$g_0(x) = \frac{\tau_m v_{eff}}{1 + \alpha} e^{-\frac{x^2}{2(1+\alpha)}} \int_x^{\sqrt{2}\Theta} dy e^{\frac{y^2}{2(1+\alpha)}} H(y - \sqrt{2}\hat{H}). \tag{E.9}$$

The firing rate v_{eff} (the zeroth order in the expansion in powers of k) is obtained by applying condition 4.17 to f_0 in equation E.5.

Similarly, while solving equation E.4, a condition over g_1 is obtained, from where g_1 is determined, except for an unknown constant D:

$$g_1(x) = D e^{-\frac{x^2}{2(1+\alpha)}} + \frac{\tau_m v_1}{1 + \alpha} e^{-\frac{x^2}{2(1+\alpha)}} \int_x^{\sqrt{2}\Theta} dy e^{\frac{y^2}{2(1+\alpha)}} H(y - \sqrt{2}\hat{H}). \tag{E.10}$$

The constant D is needed to match the boundary condition at threshold, equation 4.18.

Now it is crucial to realize that the first-order solution f_1 does not satisfy the boundary condition at threshold 4.18 for any value of D. Thus, we have to add a boundary solution f_1^b so that the total solution, equation 5.15, satisfies it up to order k. This boundary solution, found in the next section,

serves to fix the value for D as

$$D = \alpha \, v_{eff} \, \tau_m \, e^{\frac{\hat{\Theta}^2}{(1+\alpha)}}. \tag{E.11}$$

Using the normalization condition 4.17 on the term order k in the expansion of $P_\alpha(x, y)$, equation 5.15, leads to the firing rate at order k in equation 5.16.[7] In that equation, we have approximated v_{eff} by v_0, and also all α appearing in equation E.10 have been made equal to zero. These two approximations are justified because expanding v_{eff} and equation E.10 in powers of α gives corrections to the firing rate at order k that are higher than $O(\alpha)$.

E.2 The Boundary Solution. Here we find the boundary solution, f_1^b, for FPE 4.13 valid close to threshold and for small k. The FPE in this limit takes the form

$$\left[\frac{\partial^2}{\partial r^2} - \sqrt{\alpha} y \frac{\partial}{\partial r} + \frac{\partial^2}{\partial y^2} - y \frac{\partial}{\partial y} + O(k, k^2) \right] u(r, y) = 0. \tag{E.12}$$

We have replaced $f_1^b(x, y) = u(r, y) Z_0(y)$ and have made the linear transformation $r = (x - \sqrt{2}\hat{\Theta})/k$. A complete basis for this linear differential operator is not known, but if $\sqrt{\alpha} = 0$, a complete basis for an integrable function of $r \in [-\infty, 0]$, $y \in [-\infty, \infty]$ is given by the set of functions $e^{\sqrt{n}r} H_n(y/\sqrt{2})$ for all $n > 0$, where H_n are the Hermite polynomials.[8] We insert into equation E.12 a solution u of the form $u = u_0 + \sqrt{\alpha} u_1 + \alpha u_2 + O(\alpha^{3/2})$ to obtain

$$\left[\frac{\partial^2}{\partial r^2} + \frac{\partial^2}{\partial y^2} - y \frac{\partial}{\partial y} \right] u_{i+1}(r, y) = y \frac{\partial}{\partial r} u_i(r, y). \tag{E.13}$$

The solution f_1^b has to be added to the perturbative solution f_1, equation E.6, to match the boundary condition 4.18, that is,

$$De^{-\frac{\hat{\Theta}^2}{1+\alpha}} - \sqrt{\alpha} y \frac{\partial}{\partial x} g_0 \bigg|_{x=\sqrt{2}\hat{\Theta}} + u(0, y) = 0. \tag{E.14}$$

---

[7]Notice below that $\int \int u(r, z) = O(k)$, and for this reason we can neglect its contribution to the rate at order k.

[8]The Hermite polynomials satisfy the equation

$$\left(\frac{\partial^2}{\partial y^2} - y \frac{\partial}{\partial y} \right) H_n \left(\frac{y}{\sqrt{2}} \right) = -n \, H_n \left(\frac{y}{\sqrt{2}} \right).$$

The first three polynomials $H_0(y) = 1$, $H_1(y) = 2y$, and $H_2(y) = 4y^2 - 2$ are used in our calculations.

Defining $d = De^{-\frac{\Theta^2}{1+\alpha}}$ and expanding it in powers of $\sqrt{\alpha}$ as $d = d_0 + \sqrt{\alpha}d_1 + \alpha d_2 + O(\alpha^{3/2})$, as well as the others terms in equation E.14, we obtain the set of conditions

$$d_0 + u_0(0, y) = 0,$$

$$d_1 + v_{eff}\tau_m y + u_1(0, y) = 0,$$

$$d_2 + u_2(0, y) = 0.$$

Now we express each order u_i as a linear combination of the functions $e^{\sqrt{n}r} H_n(y/\sqrt{2})$, plus a particular solution as $u_i(r, y) = \sum_1^{\infty} A_{n,i} e^{\sqrt{n}r} H_n (y/\sqrt{2}) + u_{i,part}(r, y)$. We find

$$u_0 = 0, \quad d_0 = 0$$

$$u_1 = -v_{eff}\tau_m y e^r, \quad d_1 = 0$$

$$u_2 = -v_{eff}\tau_m[y^2 - 1]e^{\sqrt{2}r} + v_{eff}\tau_m[y^2 - 2]e^r, \quad d_2 = v_{eff}\tau_m.$$

With these solutions, we finally found the value of D up to order α, equation E.11.

Appendix F: Short τ_c Limit for a Generic IF Neuron

In this section we extend the formalism described in appendix E to calculate the firing rate of a generic IF neuron receiving a gaussian exponentially correlated input in the short τ_c limit (Moreno & Parga, 2002). A generic IF neuron can be defined by the leak function, $f(V)$, that determines how the voltage behaves in the absence of any input. In this model, the depolarization membrane potential $V(t)$ evolves from the reset voltage H according to the stochastic equation,

$$\dot{V}(t) = -f(V) + I(t), \tag{F.1}$$

where $I(t)$ is the synaptic current with exponentially temporal correlations as in equation 3.14. When the gaussian current is expressed using the second representation, as it is defined in section 4.2, the FPE associated with this model neuron is

$$\left[\frac{\partial}{\partial V}\left(f(V) - \mu + \frac{\sigma_w^2}{2}\frac{\partial}{\partial V} \right) + \frac{1}{\tau_c}\frac{\partial}{\partial y}\left(y + \frac{\partial}{\partial y} \right) - \sqrt{\frac{2\sigma_w^2\alpha}{\tau_c}}\frac{\partial}{\partial V} \right]$$

$$P = -\delta(V - H)J(y). \tag{F.2}$$

Using the same procedure as in appendix E, we find that the output firing rate of such a generic neuron is

$$\nu_{out} = \nu_{eff} + \nu_1 \sqrt{\tau_c} \tag{F.3}$$

where

$$\nu_{eff}^{-1} = \tau_{ref} + \frac{2}{\sigma_{eff}^2} \int_H^\Theta du\, e^{\frac{2}{\sigma_{eff}^2} \int_\Theta^u dr(f(r)-\mu)} \int_{-\infty}^u dv\, e^{-\frac{2}{\sigma_{eff}^2} \int_\Theta^v dr(f(r)-\mu)}$$

$$\nu_1 = -\frac{\sqrt{2}\alpha\nu_0^2}{\sigma_w} \int_{-\infty}^\Theta dv\, e^{-\frac{2}{\sigma_w^2} \int_\Theta^v dr(f(r)-\mu)}, \tag{F.4}$$

which is valid whenever the above integrals are defined. This general formula, which has been previously found in our work (Moreno & Parga, 2002), shows that the $\sqrt{\tau_c}$ decay of the firing rate is universal for IF models with hard threshold. Using this general formula, it is possible to obtain the firing rate in the short τ_c limit given by equation 5.16 for an LIF neuron.

Using a different procedure, we have been able to calculate exactly the firing rate of a nonleaky IF neuron ($f(V) = 0$) with exponential correlations without the need of the boundary solution to fit the boundary condition at threshold. This formula is valid for all τ_c and for small α. We still require the condition $\tau_c \ll \tau_{ref}$. This exact formula, however, allows us to check the technical procedure described above, and it naturally gives the same result. This firing rate is expressed as

$$\nu_{out} = \nu_{eff} - \frac{\alpha\nu_0^2 \left[1 - e^{(\gamma-\lambda)(\Theta-H)}\right]}{\mu(\gamma + \lambda)} + O(\alpha^2), \tag{F.5}$$

where $\gamma = \frac{\mu}{\sigma_w^2}$, $\lambda = \sqrt{\gamma^2 + \frac{2}{\sigma_w^2 \tau_c}}$ and ν_{eff} is defined below, equation F.6. An expansion of equation F.5 for small τ_c leads to the same universal $\sqrt{\tau_c}$ decay law, and the coefficients are identical to those produced by equations F.4.

$$\nu_{eff}^{-1} = \tau_{ref} + \frac{\Theta - H}{\mu}$$

$$\nu_1 = -\frac{\alpha\nu_0^2 \sigma_w}{\sqrt{2}\mu}. \tag{F.6}$$

Acknowledgments

References

Abeles, M. (1982). Role of the cortical neuron: Integrator or coincidence detector. *Isr. J. Med. Sci.*, *18*, 83–92.

Abeles, M. (1991). *Corticonics. Neural circuits of the cerebral cortex.* Cambridge: Cambridge University Press.

Aersten, A., Gerstein, M., Habib, G., & Palm, G. (1989). Dynamics of neuronal firing correlation: Modulation of "effective connectivity." *J. Neurophysiol.*, *61*, 900–917.

Albright, T. D. (1993). Cortical processing of visual motion. In F. A. Miles & J. Wallman (Eds.), *Visual motion and its role in the stabilization of gaze* (pp. 177–201). New York: Elsevier.

Amarasingham, A., Chen, T., Geman, S., Harrison, M. T., & Sheinberg, D. L. (2006). Spike count reliability and the Poisson hypothesis. *J. Neurosci.*, *26*, 801–809.

Amit, D. J., & Brunel, N. (1997a). Dynamics of a recurrent network of spiking neurons before and following learning. *Network*, *8*, 373–404.

Amit, D. J., & Brunel, N. (1997b). Model of global spontaneous activity and local structured activity during delay periods in the cerebral cortex. *Cereb. Cortex*, *7*, 237–52.

Averbeck, B. B., & Lee, D. (2004). Coding and transmission of information by neural ensembles. *Trends in Neuroscience*, *27*(4), 225–230.

Bair, W., Zohary, E., & Newsome, W. T. (2001). Correlated firing in macaque visual area MT: Time scales and relationship to behavior. *J. Neurosci.*, *21*, 1676–1697.

Bernander, O., Douglas, R. J., Martin, K. A., & Koch, C. (1991). Synaptic background activity influences spatiotemporal integration in single pyramidal cells. *Proc. Natl. Acad. Sci. USA*, *88*, 11569–11573.

Braitenberg, V., & Schüz, A. (1991). *Anatomy of the cortex: Statistics and geometry.* Berlin: Springer-Verlag.

Brunel, N., & Sergi, S. (1998). Firing frequency of leaky integrate-and-fire neurons with synaptic current dynamics. *J. Theor. Biol.*, *195*, 87–95.

Burkitt, A. N., & Clark, G. M. (1999). Analysis of integrate-and-fire neurons: Synchronization of synaptic input and spike output. *Neural Comput.*, *11*, 871–901.

Cateau, H., & Reyes, A. (2006). Relation between single neuron and population spiking statistics and effects on network activity. *Phys. Rev. Lett.*, *96*, 058101.

Compte, A., Constantinidis, C., Tegner, J., Raghavachari, S., Chafee, M. V., Goldman-Rakic, P. S., et al. (2003). Temporally irregular mnemonic persistent activity in prefrontal neurons of monkeys during a delayed response task. *J. Neurophysiol.*, *90*, 3441–3454.

Cragg, B. G. (1967). The density of synapses and neurones in the motor and visual areas of the cerebral areas. *J. Anat.*, *101*, 639–654.

Daley, D. J., & Vere-Jones, D. (1988). *An introduction to the theory of point processes.* New York: Springer.

Dean, A. F. (1981). The variability of discharge of simple cells in cat striate cortex. *Exp. Brain Res.*, *44*, 437–440.

deCharms, R. C., & Merzenich, M. M. (1996). Primary cortical representation of sounds by the coordination of action potentials. *Nature*, *381*, 610–613.

DeFelipe, J., & Fariñas, I. (1992). The pyramidal neuron of the cerebral cortex: Morphological and chemical characteristics of the synaptic inputs. *Prog. Neurobiol.*, *39*, 563–607.

Doering, C. R., Hagan, P. S., & Levermore, C. D. (1987). Bistability driven by weakly colored gaussian noise: The Fokker-Planck equation boundary layer and mean first-passage times. *Physical Review Letters*, *59*, 2129–2132.

Doiron, B., Rinzel, J., & Reyes, A. (2006). Stochastic synchronization in finite size spiking networks. *Physical Review E*, *74*, 030903.

Feng, J., & Brown, D. (2000). Impact of correlated inputs on the output of the integrate-and-fire model. *Neural Computation*, *12*, 671–692.

Fries, P., Reynolds, J. H., Rorie, A. E., & Desimone, R. (2001). Modulation of oscillatory neuronal synchronization by selective visual attention. *Science*, *291*, 1560–1563.

Fries, P., Roelfsema, P. R., Engel, A. K., König, P., & Singer, W. (1997). Synchronization of oscillatory responses in visual cortex correlates with perception in interocular rivalry. *Proc. Natl. Acad. Sci.*, *94*, 12699–12704.

Gochin, P. M., Miller, E. K., Gross, C. G., & Gerstein, G. L. (1991). Functional interactions among neurons in inferior temporal cortex of the awake macaque. *Exp. Brain Res.*, *84*, 505–516.

Kuhn, A., Aertsen, A., & Rotter, S. (2003). Higher-order statistics of input ensembles and the response of simple models neurons. *Neural Computation*, *15*, 67–101.

LaCamera, G., Rauch, A., Luscher, H.-R., Senn, W., & Fusi, S. (2004). Minimal models of adapted neuronal response to in vivo-like input currents. *Neural Computation*, *16*, 2101–2124.

Laurent, G. (2001). Odor encoding as an active, dynamical process: Experiments, computation and theory. *Ann. Rev. Neurosci.*, *24*, 263–297.

Lee, D., Port, N. L., Kruse1, W., & Georgopoulos, A. P. (1998). Variability and correlated noise in the discharge of neurons in motor and parietal areas of the primate cortex. *Journal of Neuroscience*, *18*(3), 1161–1170.

Lerchner, A., Ursta, C., Hertz, J., Ahmadi, M., Ruffiot, P., & Enemark, S. (2006). Response variability in balanced cortical networks. *Neural Computation*, *18*, 634–659.

Lindner, B. (2006). Superposition of many independent spike trains is generally not a Poisson process. *Phys. Rev. E*, *73*(2), 022901.

Lindner, B., Doiron, B., & Longtin, A. (2005). Theory of oscillatory firing induced by spatially correlated noise and delayed feedback. *Physical Review E*, *72*, 061919.

Masuda, N. (2006). Simultaneous rate-synchrony codes in populations of spiking neurons. *Neural Computation*, *18*, 45–59.

Moreno, R., & Parga, N. (2002). *Firing rate for a generic integrate-and-fire neuron with exponentially correlated input.* Berlin: Springer-Verlag.

Moreno-Bote, R., & Parga, N. (2004). Role of synaptic filtering on the firing response of simple model neurons. *Physical Review Letters*, *92*(2), 028102.

Moreno-Bote, R., & Parga, N. (2005). Membrane potential and response properties of populations of cortical neurons in the high conductance state. *Physical Review Letters*, *94*, 088103.

Moreno-Bote, R., & Parga, N. (2006). Auto- and crosscorrelograms for the spike response of leaky integrate-and-fire neurons with slow synapses. *Physical Review Letters*, *96*, 028101.

Moreno, R., de la Rocha, J., Renart, A. J., & Parga, N. (2002). Response of spiking neurons to correlated inputs. *Physical Review Letters*, *89*(28), 288101.

Nowak, L. G., Munk, M. H. J., James, A. C., Girard, P., & Bullier, J. (1999). Cross-correlation study of the temporal interactions between areas V1 and V2 of the macaque monkey. *J. Neurophysiol.*, *81*, 1057–1074.

Nykamp, D., & Tranchina, D. (2001). A population density approach that facilitates large-scale modeling of neural networks: Extension to slow inhibitory synapses. *Neural Computation*, *13*, 511–546.

Perkel, D. H., Gerstein, G. L., & Moore, G. P. (1967). Neuronal spike trains and stochastic point processes. II. Simultaneous spike trains. *Biophys. J.*, *7*, 419–440.

Renart, A., Brunel, N., & Wang, X. J. (2003). Mean-field theory of recurrent cortical networks: From irregularly spiking neurons to working memory. In J. Feng (Ed.), *Computational neuroscience: A comprehensive approach*. Boca Raton, FL: CRC Press.

Renart, A., Moreno-Bote, R., Wang, X.-J., & Parga, N. (2007). Mean-driven and fluctuation-driven persistent activity in recurrent networks. *Neural Computation*, *19*, 1–46.

Renart, A., Moreno, R., de la Rocha, J., Rolls, E., & Parga, N. (2001). A model of the IT-PF network in object working memory which includes balanced persistent activity and tuned inhibition. *Neurocomputing*, *28*, 1525–1531.

Ricciardi, L. M. (1977). *Diffusion processes and related topics in biology*. Berlin: Springer-Verlag.

Richardson, M., & Gerstner, W. (2005). Synaptic shot noise and conductance fluctuations affect the membrane voltage with equal significance. *Neural Computation*, *17*, 923–947.

Riehle, A., Grun, S., Diesmann, M., & Aertsen, A. (1997). Spike synchronization and rate modulation differentially involved in motor cortical function. *Science*, *278*, 1950–1953.

Risken, H. (1989). *The Fokker-Planck equation* (2nd ed.). Berlin: Springer-Verlag.

Rolls, E. T., & Treves, A. (1998). *Neural networks and brain function*. New York: Oxford University Press.

Rudolph, M., & Destexhe, A. (2001). Correlation detection and resonance in neural systems with distributed noise sources. *Phyical Review Letters*, *86*(16), 3662–3664.

Salinas, E., & Sejnowski, T. J. (2000). Impact of correlated synaptic input on output firing rate and variability in simple neuronal models. *J. Neurosci.*, *20*, 6193–6209.

Salinas, E., & Sejnowski, T. J. (2001). Correlated neuronal activity and the flow of neural information. *Nature Reviews Neuroscience*, *2*, 539–550.

Shadlen, M. N., & Newsome, W. T. (1998). The variable discharge of cortical neurons: Implications for connectivity, computation, and information coding. *J. Neurosci.*, *18*, 3870–3896.

Silberberg, G., Bethge, M., Markram, H., Pawelzik, K., & Tsodyks, M. (2004). Dynamics of population rate codes in ensembles of neocortical neurons. *Journal of Neurophysiology*, *91*, 704–709.

Softky, W. (1994). Submillisecond coincidence detection in active dendritic trees. *Neuroscience*, *58*, 13–41.

Softky, W., & Koch, C. (1993). The highly irregular firing of cortical cells is inconsistent with temporal integration of random EPSP's. *J. Neurosci.*, *13*, 334–350.

Steinmetz, P. N., Roy, A., Fitzgerald, P. J., Hsiao, S. S., Johnson, K. O., & Niebur, E. (2000). Attention modulates synchronized neuronal firing in primate somatosensory cortex. *Nature*, *404*, 187–190.

Stevens, C. F., & Zador, A. M. (1998). Input synchrony and the irregular firing of cortical neurons. *Nature Neurosci.*, *1*(3), 210–217.

Ts'o, D. Y., Gilbert, C. D., & Wiesel, T. N. (1986). Relationships between horizontal interactions and functional architecture in cat striate cortex as revealed by cross-correlation analysis. *J. Neuroscie.*, *6*, 1160–1170.

Tuckwell, H. C. (1988). *Introduction to theoretical neuroscience*. Cambridge: Cambridge University Press.

Usrey, W. M., & Reid, R. C. (1999). Synchronous activity in the visual system. *Annu. Rev. Physiol.*, *61*, 435–456.

Vaadia, E., Haalman, I., Abeles, M., Bergman, H., Prut, Y., Slovin, H., et al. (1995). Dynamics of neuronal interactions in monkey cortex in relation to behavioural events. *Nature*, *373*, 515–518.

Wehr, M., & Laurent, G. (1999). Relationship between afferent and central temporal patterns in the locust olfactory system. *J. Neurosci.*, *19*, 381–390.

White, E. L. (1989). Cortical circuits. New York: Birkauser.

Zohary, E., Shadlen, M. N., & Newsome, W. T. (1994). Correlated neuronal discharge rate and its implication for psychophysical performance. *Nature*, *370*, 140–143.